Disease Risk Forecasting with Bayesian Learning Networks: Application to Grape Powdery Mildew (*Erysiphe nector*) in Vineyards

Weixun Lu, Nathaniel K. Newlands, Odile Carisse, David E. Atkinson, & Alex J. Cannon

April 2020

agronomy

MDPI

Article

Disease Risk Forecasting with Bayesian Learning Networks: Application to Grape Powdery Mildew (*Erysiphe necator*) in Vineyards

Weixun Lu [1], Nathaniel K. Newlands [2,*], Odile Carisse [3], David E. Atkinson [1] and Alex J. Cannon [4]

1 Department of Geography, University of Victoria, David Turpin Building, 3800 Finnerty Road, Victoria, BC V9P 5C2, Canada; lu@uvic.ca (W.L.); datkins@uvic.ca (D.E.A.)
2 Science and Technology, Agriculture and Agri-Food Canada, Summerland Research and Development Centre, 4200 Highway 97 S, P.O. Box 5000, Summerland, BC V0H 1Z0, Canada
3 Science and Technology, Agriculture and Agri-Food Canada, Saint-Jean-sur-Richelieu Research and Development Centre, 430 Gouin Boulevard, Saint-Jean-sur-Richelieu, QC J3B 3E6, Canada; odile.carisse@canada.ca
4 Climate Research Division, Environment and Climate Change Canada, 3800 Finnerty Road, Victoria, BC V8P 5C2, Canada; alex.cannon@canada.ca
* Correspondence: nathaniel.newlands@canada.ca

Received: 14 March 2020; Accepted: 17 April 2020; Published: 28 April 2020

Abstract: Powdery mildew (*Erysiphe necator*) is a fungal disease causing significant loss of grape yield in commercial vineyards. The rate of development of this disease varies annually and is driven by complex interactions between the pathogen, its host, and environmental conditions. The long term impacts of weather and climate variability on disease development is not well understood, making the development of efficient and durable strategies for disease management challenging, especially under northern conditions. We present a probabilistic, Bayesian learning network model to explore the complex causal interactions between environment, pathogen, and host for three different susceptible northern grape cultivars in Quebec, Canada. This approach combines environmental (weather, climate), pathogen (development stages), and host (crop cultivar-specific susceptibility) factors. The model is evaluated in an operational forecast mode with supervised and algorithm model learning and integrating Global Forecast System (GFS) Ensemble Reforecasts (GEFSR). A model-guided fungicide spray strategy is validated for guiding spray decisions up to 6 days with a 10-day forecast of potential spray efficacy under rain washed off conditions. The model-guided strategy improves fungicide spray decisions; decreasing the number of sprays, and identifying the optimal time to spray to increase spray effectiveness.

Keywords: Bayesian learning networks; forecasting; modeling; powdery mildew disease; risk; viticulture

1. Introduction

1.1. Economic Importance of Grapes in North America

Grapevine growers across North America grow a wide range of grapes, mostly producing table grapes, raisins, and wines. Grapes and their derivative products represent a significant contribution to the economy of North America. As reported for 2015 in California, the primary U.S. wine-grape growing region, grapes and their derivative products contributed $57.6 billion to the state's economy and $114.1 billion to the U.S. economy. In Canada, grapes are produced primarily in Ontario (66%

of acreage), British Columbia (33% of acreage), Quebec (5% of acreage), and Nova Scotia (3% of acreage). In 2015, the Canadian wine and grape industry contributed $9 billion to the Canadian national economy, with the province of Quebec contributing $1 billion [1].

The grapevine production areas in Quebec are characterized by very cold winter temperatures as low as −30 °C to −35 °C, a cold and wet spring, hot summers, followed by potentially a cold fall. This climate influences the selection of grape varieties and the type of wine to be produced. In this climate berries can reach maturity within the period without frost (i.e., bud emergence after latest spring frosts and berry ripening prior to the first killing frost in the fall) and survive cold winter conditions [2]. Most grapevines are still protected during the winter months with soil or geotextiles [2]. In the spring, such winter protection is removed after the last risk of spring frost to prevent frost damages to primary and secondary flower buds [3]. These conditions influence both grapevine growth and disease development. The grapevine development cycle is characterized by rapid vegetative growth from late May to end of July, follow by slower growth in August and September. The northern climate also influences grape diseases including powdery mildew caused by *Eriysphe necator* (Schw.) Burr., (synonym *Uncinula necator*). Powdery mildew (hereafter, PM) progresses slowly from late May to end of July and rapidly in August and September. Hence PM incidence, when expressed as the proportion of disease leaves is very low, until generally late July to early August, constraining earlier scouting and disease forecasting.

1.2. Grape Powdery Mildew (PM) Disease

Grape PM caused by *Eriysphe necator* (Schw.) Burr., (synonym *Uncinula necator*) is an obligate parasite affecting only plants in the genus *Vitis*. For more than 150 years, PM has been a significant challenge for grape production [4]. Since the 1850s, research on this disease has been undertaken in response to several major epidemics in Europe. The disease causes both direct (crop losses) and indirect (reduced vine vigor) damages. Moderate to severe disease epidemics cause reduced yield (lower berry weight), delayed berry maturity, and altered wine composition and sensory characters [5–7]. Current guidance for disease mitigation calls for the application of fungicide sprays at a repeating 7 to 14 days interval. This approach tends to be of limited effectiveness as it does not consider the complex interaction between this pathogen and its host in relation to local weather and broader, regional climate variability. Over-spray is costly and harmful as the chemical can remain on berries, and the local environment. Effective management of grape PM requires the development of efficient and durable strategies to fine-tune fungicide application timings and amounts, taking into account the effect of environmental variability on disease development and pathogen dispersal.

The complex interactions between the pathogen and the host, influenced by climate and weather, drives the rate of PM development and its impact severity. Growth stage (ontogenic resistance) [8,9] and grape cultivar genetics both influence grapevine susceptibility to this disease. Cultural practices that favor vegetative vigor may predispose the host to an increased development of PM. High grapevine vigor can also modify ontogenic resistance of leaves, delaying grapevine phenological stages such as veraison or harvest, or stretching the duration of the flowering, fruit set, or bunch closure periods [10]. Grape PM can affect all above-ground parts of grapevine. A typical disease progression begins on the leaves, where lesions found on the undersides of leaves are the first visual indication of an infection. As the disease progresses, lesions become apparent on the upper sides of the leaves as well. In the absence of control, these lesions will increase both in size and number, causing premature leaf drop. On shoots, symptoms are brown to black irregular lesions that vary in size. On inflorescences and rachis, PM has the appearance of a grey to whitish powder. Severe infections of the rachis can result in premature drop of clusters. The disease can attack berries immediately after bloom through four weeks post-bloom. Infected berries are ash grey and quickly become covered with spores, giving them a floury appearance. Berries infected later during the period of susceptibility are prone to splitting, making them susceptible to infection by other grapevine pathogens [11].

1.3. Impacts of Climate on Grape Powdery Mildew

PM is a polycyclic disease that evolves in two distinct phases: the primary infection, caused by ascospores (sexual spores), and secondary infections, caused by conidia (asexual spores). Its epidemiology is well-studied [6,12–20]. The pathogen overwinters as cleistothecia which contain immature ascospores. In Eastern Canada, the cleistothecia are the likely source of primary inoculum. Dehiscence of the cleistothecia commonly starts at bud break and continues until the beginning of flowering [14]. Ascospores are released from cleistothecia in response to rain (greater than 2.5 mm) when the temperatures are between 6 and 24 °C; infection will not occur outside of this temperature range. Once released, ascospores that fall on young leaves cause the primary infections. Ascospore germination requires free water or high relative humidity. Infection takes place within an optimal temperature range of 20 to 25 °C, if there is sufficiently high leaf wetness over a duration of 4 h. Once an infection is established, lesions will develop on infected leaves within 6 to 30 days, depending on temperature variability. Potentially large amounts of conidia are produced on these lesions. They are primarily dispersed by the wind [18,19,21,22]. Unlike ascospores, conidia do not need free water for germination. Their germination is controlled by temperature, relative humidity, and light intensity. The optimal temperature for germination of conidia is 25 °C [23]. Most conidia germinate at a relative humidity of 40 to 100%. Relative humidity is often not a limiting factor for germination [24]. At temperatures of 23 to 30 °C, secondary infection cycles can be completed within 5 to 7 days [25]. At the end of the growing season, cleistothecia appear on infected leaves and berries. Vineyards are more likely to experience a severe damage (and suffer more extensive damage) if the initial infection occurs early in the season with temperatures suitable for the development of the initial lesion and ensuing conidia outbreak.

1.4. Management of Grape Powdery Mildew

Current PM disease control strategies consist almost exclusively of schedule-based fungicide spray applications, involving grape growers regularly applying fungicide spray under constant or regular time intervals (e.g., ranging from 7 to 21 days) from the beginning to the end of the growing season. This is generally effective in managing PM disease, but raises production costs, promotes fungicide resistance, and can be detrimental to both human and environmental health. There have been numerous attempts to link spray application timing and fungicide selection to climate and environmental information. The Gubler–Thomas program, developed at University of California (UC)-Davis (http://ipm.ucanr.edu/DISEASE/DATABASE/grapepowderymildew.html), was designed to create a disease risk index using daily average temperature and measured leaf wetness hours for both ascospores and conidial infections to guide fungicide spray strategies for several widely-used fungicide products (i.e., sulfur dust, micronized sulfur, and DeMethylation Inhibitor (DMI) fungicides).

The impact of PM on grape yield loss is closely related to the severity of conidial infection on both leaves and berries. Thus, application of fungicide spray when the first conidia infection occurs, can intercept and stop a disease outbreak before it can establish itself. This spray timing can also reduce the total number of applications required over a growing season and, in turn, spray costs. Caffi et al. (2011) developed a mechanistic model to predict the initiation time of a conidia infection using stochastic and dynamic process models of the lifecycle of overwintered ascospore, as influenced by daily weather conditions [26]. This model was validated over four years (2005–2008) in 26 vineyards in Italy and had a 94% accuracy in correctly predicting outbreaks. The host-pathogen model of Calonnec et al. (2008) provides spatial and temporal dispersal information of conidial infections in relation to factors such as the number, age, and pattern of healthy and infected organs, infectious leaf area, and the density of spores released [27].

The Gubler–Thomas program has become a primary disease management tool in California for grape disease control, but is not well-suited for PM disease control in Quebec because of this region's climate variability [21]. Instead, a model based on degree-days, developed by Carisse et al. (2009) and

has been shown to reduce the number of spray applications by up to 55%, by determining the initial date to start the application of fungicide spray. This initial date matches the Eichhorn–Lorenz grape phenological stage 7 which is the stage in plant development when there are 2–3 young leaves fully expanded from shoot tips. The model is currently operationally deployed across Quebec and attains a disease control efficiency similar to that of a calendar/schedule-based fungicide program based on regular intervals rather than a model-based schedule [21,22].

1.5. Problem Statement

PM management tools have primarily been developed for temperate climate grapevine production areas. More complex, multi-variate models are needed to improve our understanding of PM epidemiology under northern climate and to improve the accuracy of model-based forecasting of the optimal timing of fungicide application. While schedule-based programs can help to significantly reduce the frequency of fungicide sprays over a growing season, contact fungicides are susceptible to being washed off when cumulative rainfall or irrigation after a fungicide spray reaches 25 mm or more. This is a major issue that many existing fungicide spray programs do not consider. Models also need to consider how the efficacy of fungicide spray impacts PM epidemiology over longer time frames. An improved model-guided approach to PM management is needed that can be implemented operationally by grape producers to reduce production costs and environmental (i.e., weather and climate-related) risks. A model-guided approach could increase the long-term economic and environmental sustainability of viticulture under current and future climate.

1.6. Research Objective

The primary research objective is to develop a probabilistic model that can provide reliable forecasting of PM risk to guide fungicide spray strategies under local weather conditions and changing regional climate variability. Such a model needs to include relevant measurement parameters and variables, so that it can be calibrated and operational deployed in vineyards. It also needs to integrate weather and climate information in near-real-time (NRT) in order to ensure fungicide management is more effective, efficient, and less costly. We present a novel probabilistic model (i.e., Bayesian network model) developed to forecast the risk of PM, validating it against experimental data from Quebec, Canada for three northern grape cultivars—Chancellor, Geisenheim-318-57 (Vitis International Variety Catalogue: http://www.vivc.de/index.php?r=passport%2Fview&id=4710), (hereafter, Geisenheim-318), and Frontenac. These cultivars represent high, medium, and low susceptibilities to PM, respectively. The model combines information from observational data and climate models, integrating climate, host stage, cultivar and autoregressive life-cycle process considerations, and factors involved in their complex interaction. The model is tested under two competing learning modes (i.e., supervised and algorithm) that alters the model's structure (i.e., association of factors and the strength of their influence). This network learning generates insights on essential variables and complex interactions that exist for specific sites (i.e., vineyard ecosystems). By using both structural and parameter optimization, and allowing the model to determine the best model design in a probabilistic and dynamic way, this approach extends existing, mechanistic methods. Such methods typically consider far fewer possible variables/factors, are static, and are calibrated by tuning a fixed number of parameters so are difficult to be applied across different sites and regions, and do not have the ability to predict dynamics, nor generate future forecasts. The forecast-skill of the best-performing model in predicting disease risk or future disease incidence is assessed using Global Forecast System (GFS) Ensemble Reforecasts [28]. GFS Ensemble Reforecast (GEFSR) provides an 11-member ensemble of historical reforecasts and real-time forecasts of weather conditions with lead times of up to 16 days. A model-based fungicide spray program providing up to 10 days of forecast disease incidence with fungicide application guidance for up to 6 days is showcased driven by GEFSR weather forecasts.

2. Materials and Methods

2.1. Study Site

The study site was the Agriculture and Agri-Food Canada (AAFC) experimental farm located in Frelighsburg, Quebec, Canada (lat. 45.05° N and long. 72.86° W) (Figure 1). Grapevines are arranged in spatial grid units with 3 m × 0.9 m (*row* × *column*). Hourly climate data, including temperature, wind velocity, relative humidity, and rain intensity, were monitored at the canopy level (around 1.5 m height) within the grapevine canopy and collected through the growing season (May–September) from 2000–2011. The lower part of Chancellor and Geisenheim-318 were covered with 40–60 cm of soil during winter seasons, and the soil was removed at the beginning of the next growing season. Disease sprays (other than PM) for downy mildew and Botrytis bunch rot and insecticides to control flea beetle were applied. Other cultural practices were performed according to standard commercial viticulture practices. PM disease incidence (hereafter, DI) was measured as the ratio of infected leaves over the total number of sampled leaves. PM incidence (hereafter, DI) was assessed twice weekly from bud break (mid-May) until harvest (mid to late September) by looking at two shoots on eight vines per plot, selected randomly each time. At each sampling time, the total number of leaves and total diseased leaves were recorded. A leaf was considered to be diseased if it had one or more lesions. DI was used as the response variable instead of disease severity because visual estimation of severity, expressed as the proportion of leaf area diseased, is very difficult and not sufficiently reliable when done under field conditions.

The variability of seasonal climate (May to September) and DI for grape PM for each of the three susceptible cultivars is shown (Figure 2). Typically, summer temperature at the experimental farm varied between 15 °C in May to a maximum of around 20 °C in July and August, reducing slightly to around 15 °C in September. Daily temperatures from July to September varied from a minimum of 10 °C to a maximum of around 27 °C, which is suitable for infections of both ascospore and conidia. Summertime at the experimental farm was humid with many rainfalls. Daily rainfall totals of over 25mm were recorded. Daily relative humidity varied between 60 to 95%, with an average value of around 70% from July to September. Daily wind speed varied from as low as 2 km/h up to around 20 km/h, with average wind speed around 7 km/h. The local weather and regional climate conditions at this site are suitable for the development of grape PM, but vary enough that standard spray regimes (based on fixed interval or basic weather-guided protocols) cannot provide adequate protection. Suitable temperatures and frequent rainfalls early in the growing season causes ascospore to be released from over-wintered cleistothecia during a bud-break and dispersed within the vineyard over distances that depend on the prevailing wind conditions. Applied fungicide is also washed off by frequency and/or intense rainfalls, leading to high DI, even if a regular spray regime is followed.

Measured DI for the northern grape cultivars vary with weather and climate, exhibiting different levels of susceptibility (Figure 2). Although disease monitoring starts in May, the first signs of infection are detected in the beginning of July. DI increases rapidly in August, reaching a peak in mid-September, then decreasing until the end of the growing season. The maximum DI over a growing season is dependent on the timing of disease outbreak (Figure 3). Earlier disease outbreaks result in higher DI in some years (i.e., 2001 and 2010); the reverse pattern was also observed in other years (i.e., 2004 and 2009).

Figure 1. The experimental farm (top) and the weather station (bottom) used to monitor climate variables at the grape canopy level from 2000 to 2011.

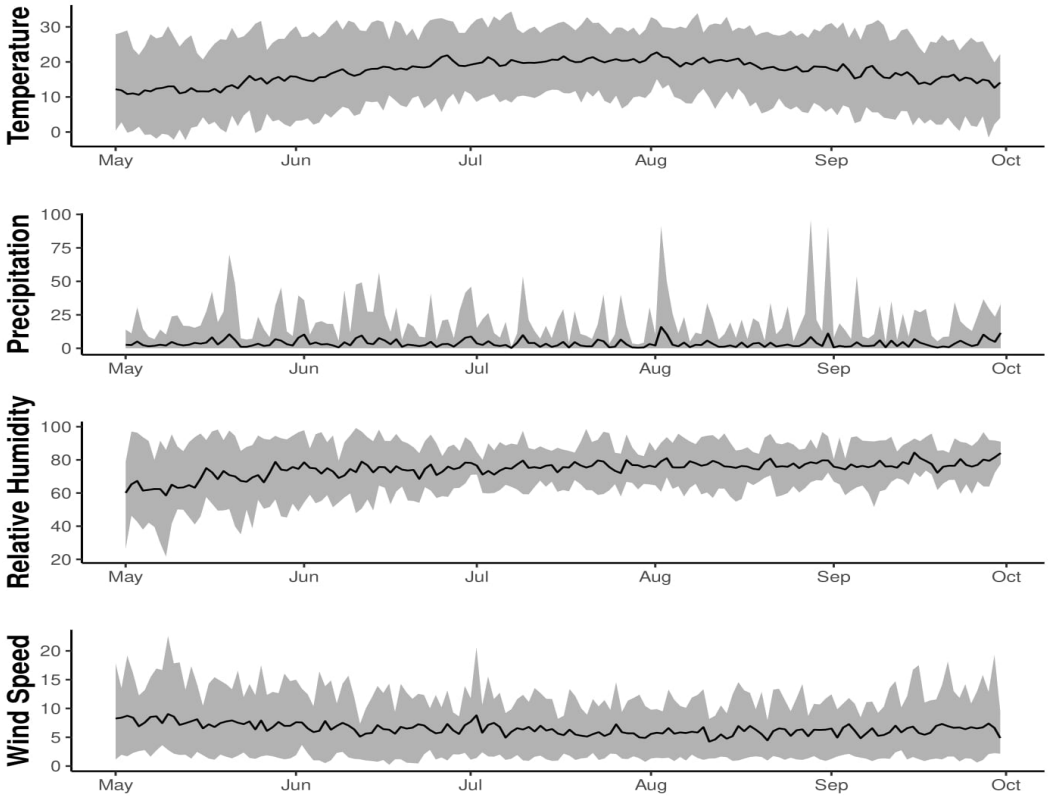

Figure 2. *Cont.*

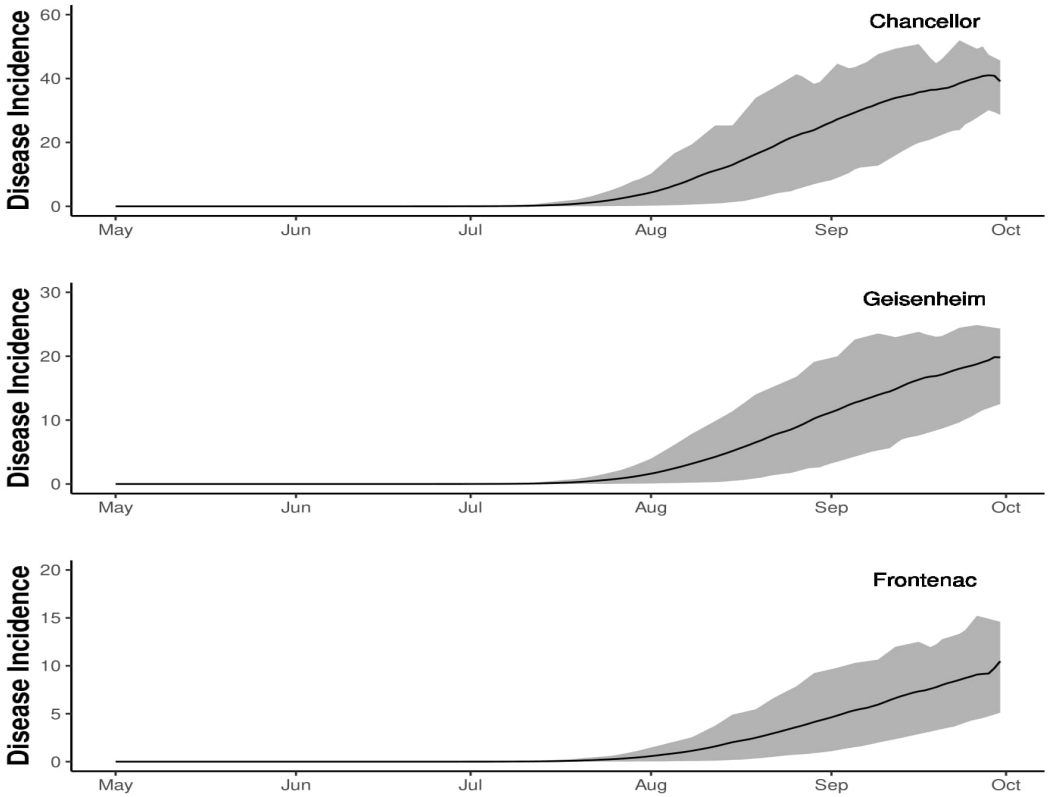

Figure 2. Seasonal climate variability and disease incidence (DI) (% infected/non-infected leaves) of grape powdery mildew (PM) through the growing season for northern hybrid grape cultivars with differing susceptibility (Chancellor, Geisenheim-318, Frontenac). The mean (solid line) is shown varying between minimum (lower bound) and maximum (upper bound) observed values (2000–2011).

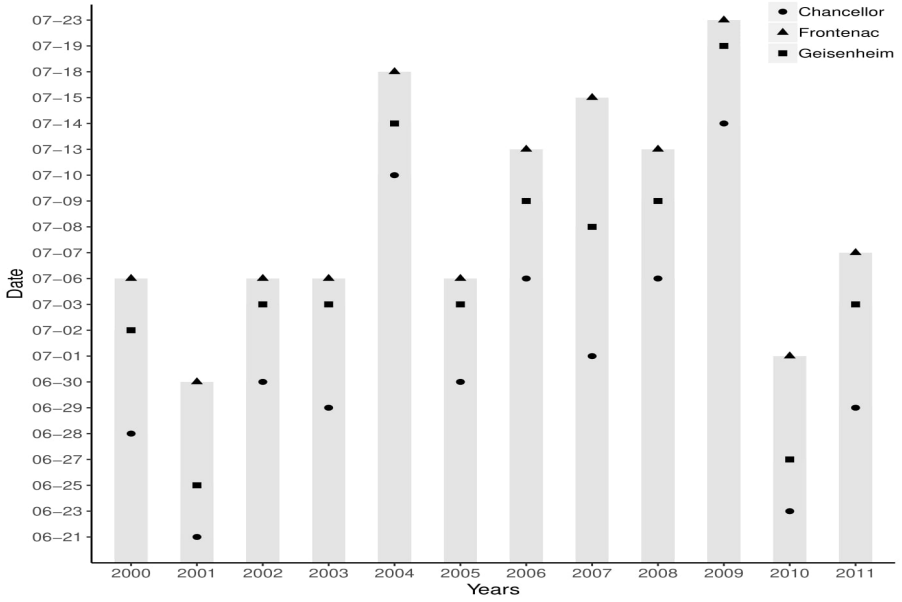

Figure 3. *Cont.*

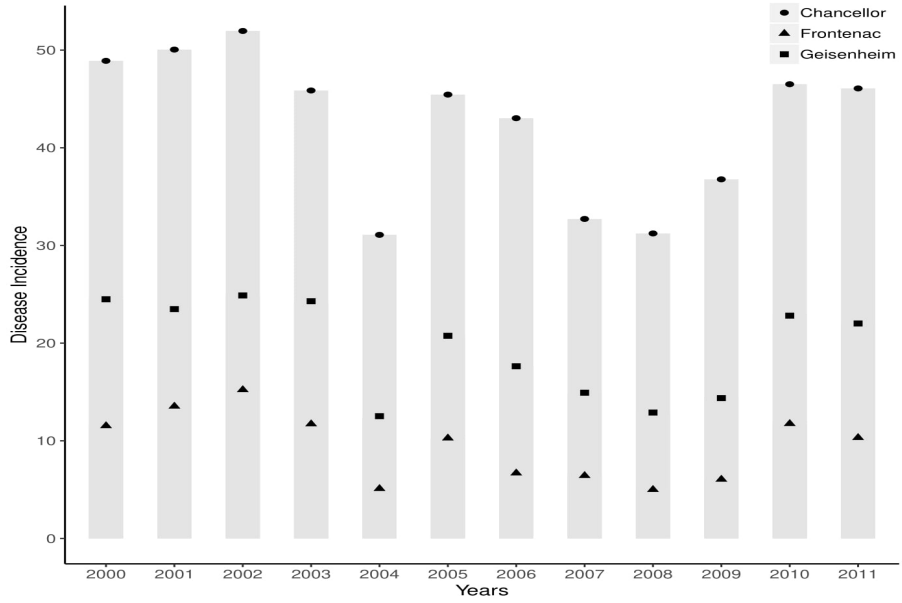

Figure 3. Annual first disease date (top) and the maximum DI (bottom) of grape PM for the three susceptible cultivars: Chancellor (circle); Geisenheim-318 (square); and Frontenac (triangle).

2.2. Global Forecast System (GFS) Ensemble Reforecasts (GEFSR)

Reforecasts, also known as hindcasts, are retrospective numerical weather prediction (NWP) forecasts made for extended periods using a fixed version of a weather forecast model and data assimilation system. Ideally, the reforecast NWP system is the same as one that has been used operationally. Reforecasts provide valuable data for developing statistical forecast models for environmental variables. The availability of an extended, relatively homogeneous reforecast dataset—one that matches the statistical characteristics of an operational forecast system—allows robust calibration of statistical forecast model parameters.

The US National Oceanic and Atmospheric Administration (NOAA)'s 2nd. generation GEFSR dataset provides meteorological variables used as predictors in the disease risk forecast model [28]. GEFSR produces retrospective ensemble NWP forecasts every day at 0000 UTC using the National Centers for Environmental Prediction (NCEP) Global Ensemble Forecast System (GEFS) (version 9.0.1 ca. 2012). GEFS is one of the models that contributes to the North American Ensemble Forecast System (NAEFS). This is a joint project to provide long-range, probabilistic weather forecasts by the national weather services of Canada, United States, and Mexico. The GEFSR ensemble consists of 1 control forecast and 10 perturbed ensemble members, with archived reforecasts available from December 1984 until the present. Reforecasts are recorded at 3-hourly intervals for lead times from 0 to 72 h and at 6-hourly intervals after 72 h. During the first 8 days of the GEFS reforecasts, the model is run at T254L42 resolution (equivalent grid spacing of 40 km at 40 degrees latitude and 42 vertical levels). From 8 to 16 days, the model is run at T190L42 resolution (54 km horizontal grid spacing). Reforecasts from GEFSR are statistically consistent with forecasts from the operational 00 UTC run of GEFS [28]. All model predictors are ensemble averages over the 11 forecast members. For PM disease risk forecasting, a set of available reforecasted weather and climate variables were selected from the GEFSR archive (i.e., minimum temperature, maximum temperature, total precipitation, sea-level pressure, specific humidity, U-component, and V-component wind speed (near-surface)), with relative humidity computed from specific humidity and sea-level pressure.

2.3. Grapevine Development

The model assumes the susceptibility of grapevines to PM is variable through a growing season. The development of grapevines can be divided into five stages using interval values from the commonly

used plant growth index called Cumulative Growing Degree Days (CGDD). CGDD is a cumulative sum of daily growing degree days (GDD) calculated by the daily temperature degree above a specific base temperature (T_{base}), usually taking values between 0 °C and 10 °C [29–31], a base temperature of 10 °C is mostly used for grapevines [32,33]. CGDD is given by,

$$CGDD_i = \sum_i (T_i - T_{base}) \tag{1}$$

where T_i is the daily mean temperature calculated as the average value between the daily maximum and minimum temperature. Accumulation of daily values starts on April 1st for a given growing season. The specific phases of grapevine are defined as: *Off-Season* ($CGDD < 20$), *Bud break* ($20 \geq CGDD < 254$), *Flowering* ($254 \geq CGDD < 680$), *Setting* ($680 \geq CGDD < 1100$), and *Veraison* ($1100 \geq GDD$).

2.4. PM Disease Development

The development of grape PM is highly dependent on grapevine development, local weather conditions, and regional climate variability. Empirical equations that track the development of grape PM were calibrated and validated for our study site for later integration into our probabilistic forecast model. Parameter estimates were either tuned or fixed based on published scientific literature and internal Agriculture and Agri-Food Canada (AAFC) reports. It was assumed that the pathogen over its life-cycle has the same temperature response to changing daily temperature, but the time (days) it takes to complete a full development cycle can change, such that some spore development phases may take more than a day to be completed under optimal climate conditions.

A temperature effect rate function was specified to relate the daily rate of PM development (as a percentage) to daily mean temperature. The temperature effect rate function is the inverse of the latent period equation [34,35].

$$\theta(T) = \begin{cases} \frac{15}{138-7T} & 6\,^{\circ}\text{C} \leq T < 17\,^{\circ}\text{C} \\ \frac{(m+n)^{(m+n)}}{n^n m^m} T_n^n (1-T_n)^m & 17\,^{\circ}\text{C} \leq T \leq 32\,^{\circ}\text{C} \end{cases} \tag{2}$$

with,

$$T_n = \frac{T - T_{min}}{T_{max} - T_{min}} \tag{3}$$

where T is the daily mean temperature. T_{max} and T_{min} are the temperatures at maximum and minimum thresholds for either mycelial growth or spore infection, respectively. $\theta(T)$ equals zero when $T \leq 6\,^{\circ}$C or $T > 32\,^{\circ}$C. It was validated with AAFC data on the number of days required to complete a latent period under varying daily temperatures. PM development rapidly increases when the temperature is between 6 °C and 17 °C because the curve of the effect rate function is concave up (Figure 4). The rate of temperature effect is high (above 75%) when the temperature is between 17 °C and 31 °C, and reaches a peak when daily mean temperature at 26 °C matches the optimal temperature for PM development. The rate of temperature effect then drops at higher temperatures.

The cumulative proportion of ascospores ready for release (PAR) is a proportion of over-wintered ascospores within a vineyard and is computed as a function related to CGDD from Equation (1). We assume that the vineyard has the same amount of over-wintered ascospores population, N, every year, so that N can be omitted from the computation, and the primary infection caused by ascospores would only depend on the values of PAR. The equation of PAR is:

$$PAR_i = \exp[-\alpha \cdot \exp(-\beta \cdot CGDD_i/100)] \tag{4}$$

where $CGDD_i$ is the Cumulative Growing Degree Days for day i. The proportion of PAR is a rate value that falls into an interval of $[0, 1]$. The process of ascospore release is considered to have stopped

when PAR reaches 1. Equation (4) was first introduced for ascospores infection modeling at the bud break stage [26]. The daily rate of ascospore maturation (AMR) is calculated as the daily change of PAR within the day in $(i-1, i)$ and is expressed as the daily rate of ascospores ready for release.

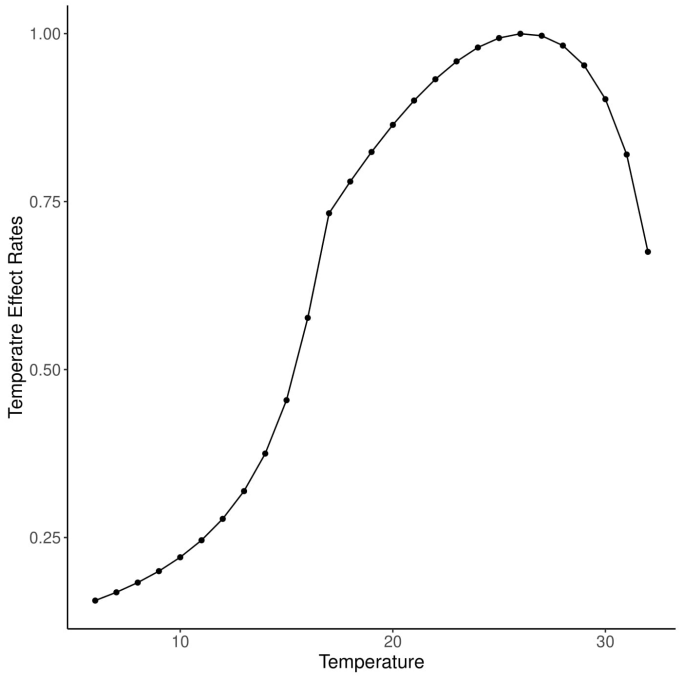

Figure 4. Temperature effect rate plot of the developing rate of PM in response to daily temperatures from 6 °C to 32 °C.

Ascospores released from leaves during the AMR stage will germinate when there is at least 2 mm of rainfall R_i [14,36], and the daily temperature is between $6\,^{\circ}\text{C} \geq T \leq 31\,^{\circ}\text{C}$ [21,22,27]. The germination rate of ascospores ADR depends on the leaf wetness duration in hours (WD) and canopy temperature (T). Caffi et al. (2011), using data from Gadoury et al. (1990) derived the following ascospore germination rate equation (ADR) [14,26],

$$ADR_i = 1 - \delta \cdot \exp(-\lambda \cdot T_i^2 \cdot WD_i) \tag{5}$$

where $R_i \geq 2$ mm and T is the daily mean temperature with $4\,^{\circ}\text{C} \leq T < 30\,^{\circ}\text{C}$. $ADR_i = 0$ otherwise. Through the process of germination, released ascospores are transferred into ungerminated (AUG) and germinated (AOG) ascospores. AUG spores remain on the leaf leave and wait for the next germination opportunity when environmental conditions are suitable, and AOG is preparing for primary infection. The equations of AUG and AOG depend on the amount of ungerminated ascospore at day $(i-1)$, the amount of newly released ascospores, and germination rate at day i.

$$AUG_i = (AUG_{i-1} + AMR_i) \cdot (1 - ADR_i) \tag{6}$$

$$AOG_i = (AUG_{i-1} + AMR_i) \cdot ADR_i \tag{7}$$

The primary infection rate (PIR) at any given day i can be calculated as a function of Equations (2) and (7):

$$PIR_i = AOG_i \cdot \theta(T) \tag{8}$$

where $\theta(T)$ is computed from Equation (2). Once primary infection has occurred, lesions are generated on infected leaves to produce conidia following a latent period $\rho(t)$. The latent period $\rho(t)$ was

calculated using the minimum time (days) required to complete a latent period and the daily temperature effect rate from Equation (2) [27,35,37]. The latent period equation is:

$$\rho(T) = \begin{cases} 46 - \frac{7}{3 \cdot T} & 6\,^{\circ}\mathrm{C} \leq T < 17\,^{\circ}\mathrm{C} \\ \frac{\rho_{min}}{\theta(T)} & 17\,^{\circ}\mathrm{C} \leq T \leq 32\,^{\circ}\mathrm{C} \end{cases} \tag{9}$$

A latent period is considered complete when $\sum[1/\rho(T)] = 1$; this releases a large amount of conidia spores for dispersal, which cause the secondary infection. Figure 5 shows the latent period response to temperature described by Equation (9) (solid line), calibrated to parameter estimates from the AAFC vineyard data.

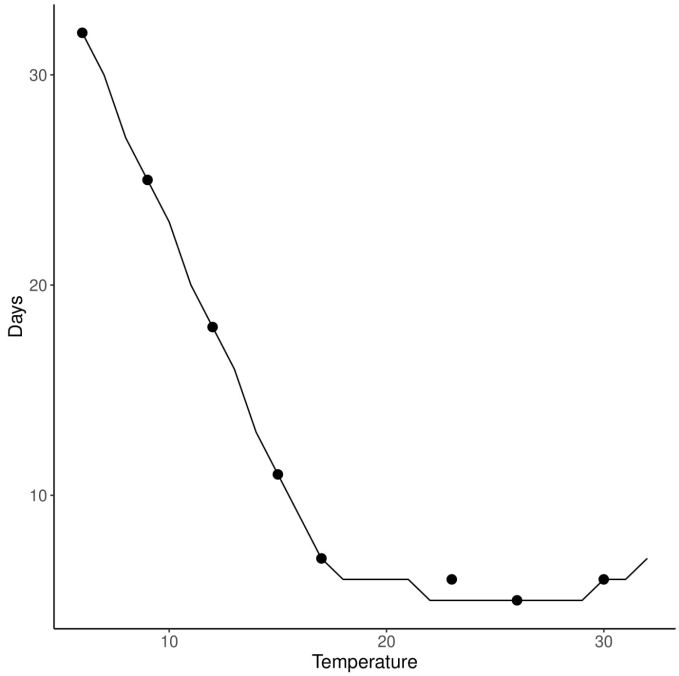

Figure 5. Number of days needed to complete a latent period responses to daily temperatures (°C). The solid line represents the estimated time to complete a latent period from Equation (9) in relation to measured days to complete a latent period.

The spatial dispersal of conidia depends on the condition of wind. Willocquet et al. (1998) provide a dispersal rate equation of conidia spore using wind duration, wind speed, and the ages in days of the lesions [19]. The dispersal rate (DR) equation is:

$$DR = \exp(r \times u + b)/(1 + \exp(r \times u + b)) \tag{10}$$

where u is the daily wind speed (km/h). r and b are the parameters of the equation. Values of r and b vary depending on the age of a lesion [19]. The infection by conidia is a rain-free process and depends only on daily temperature. The daily infection rate of conidia secondary infection rate (SIR) can be expressed as a function of the temperature effect rate from Equation (2). Calonnec et al. (2008) indicate that there is a maximum threshold of around 53% of the total conidia spores that can cause infection on leaves given optimal temperature condition [27]. SIR is given by,

$$SIR = I_0 \cdot \theta(T) \tag{11}$$

where $\theta(T)$ is from Equation (2), and T_0 is the maximum daily infection threshold of conidia under optimal temperature, $T_0 = 0.53$. Infection of conidia starts from the day of the first completed latent period, which is the day of conidia dispersal starts, until the end of the growing season.

Table 1 provides the values and detailed descriptions of the equation parameters. Factors retained for inclusion in the network modeling of disease risk of grape PM include: primary infection PIR, secondary infection SIR, the daily number of completed latent periods LP, and dispersal rate DR.

Table 1. Calibrated, site-specific parameter values for PM model.

Parameter	Description	Equation	Values	Reference
n_I, m_I	Shape parameters	(2)	1.055–0.338	[34,35]
T_{max}, T_{min}	Temperature thresholds for pathogen infection	(2)	33–5 (°C)	[23,38]
n_g, m_g	Shape parameters	(2)	1.24–0.27	[34,35]
T_{max}, T_{min}	Temperature threshold for latent period	(2)	33–5 (°C)	[34,35]
α, β	Location parameter, growth rate parameter	(4)	1.95–1.91	[26]
δ, λ	Location parameter, growth rate parameter	(5)	0.969–0.0004	[26]
ρ_{min}	Minimum time to complete a latent period	(9)	5 (days)	AAFC
I_0	Maximum infection rate	(11)	0.53	[27]
r, b	Spore dispersal rate by wind, capacity rate of a lesion to withhold conidia	(10)	(Table 2)	[19]

3. Bayesian Network Learning Model

Bayesian networks (BNs), also known as belief networks, are directed acyclic graphical (DAG) probabilistic models that are widely used to represent the complex joint probability distributions between network variables. The complex causal relationships between random variables X_i are split into multiple local distributions and represented as a DAG. Independent random variables within a DAG are represented as nodes. They are linked by edges from the direct causes as determined by the conditional dependencies probability P. Each variable is conditionally dependent on its effects and independent of its non-effects. Conditional dependencies can be estimated either by using statistical and computational methods or incorporation of expert experience. Let X denoted as a set of random variables in a DAG, then the full joint probability distribution has expressed as:

$$P(X) = P(x_1, x_2, \ldots, x_n) = \prod_{i=1}^{n} P(x_i|\pi_i) \quad (12)$$

where x_i and π_i, $i = 1, 2, \ldots, n$, are child and parent nodes, respectively. The distribution of child nodes depends only on their parent nodes, the number of which is limited. The global joint distribution is split into local distributions. The forecast model was coded and implemented using the statistical programming language R (version 3.4.2) making use of validated, open-source algorithm libraries: bnlearn (structure learning), mltool (calculating MSE), and other plotting packages (i.e., Rgraphviz, graph, plot3D, ggplot2, RColorBrewer).

3.1. Supervised and Algorithm Learning

Fitting a Bayesian network to data, usually called learning has two forms: structural learning and inference learning. Structural learning also has various forms, and can be based on expert knowledge, termed supervised learning, or based on statistical or computational learning algorithms, termed algorithmic learning. This later approach uses multiple learning algorithms to link random variables within a network into a DAG. Random variables within a network can be discrete, continuous, or hybrid data types, where hybrid is a network containing both discrete and continuous random variables. In a hybrid Bayesian network, network learning to establish causal relationships proceeds under certain restrictions: a child of continuous data type can have either discrete or continuous data type parent nodes, but a child of discrete data type must have discrete parent nodes. This logical connection between child and parent nodes helps to avoid linking problems in structure learning, providing better estimations for parameter learning.

Both supervised and algorithmic learned were employed for the Bayesian network to learn the complex interactions between a grapevine and PM disease under varying environmental conditions. For the supervised learning, the causal relationships within the Bayesian network were linked to the calibrated empirically-derived equations described previously in Sections 2.3 and 2.4.

The grape PM risk assessment model, P_{maxacc} [21], was used to specify airborne conidium concentration for structural learning of the model. This model is developed from the Richards model using CGDD based on a 6 °C threshold. The Richards model was selected because it had used the observations from the same experimental farm site in this study, which was responsible for reducing fungicide spray for disease control by as much as 40% from 2004 to 2007. We examined the Pearson correlations between the DI for the three susceptible grape cultivars. The PM risk assessment model had different base temperatures ranging from 1 °C to 13 °C. A temperature of 3 °C was selected as the base temperature because it had the highest value in the correlations. The PM risk assessment model is:

$$P_{maxacc} = 1.0755(1 + e^{-0.0042 \times CGDD})^{1/(1-1.0169)} \quad (13)$$

where $CGDD$ is the cumulative growing degree days from Equation (1).

Numerous approaches exist for implementing algorithm learning, with the two main approaches being constraint-based and score-based learning. Constraint-based learning involves developing relationships based on the framework from [39], which uses a conditional independence test inductive causation (IC) to learn the Bayesian network structure. Structural learning involves determining the so-called Markov blanket of each node in the network and is defined as containing the only knowledge needed to predict the behavior of a node and its children within a larger network. Learning algorithms include the Grow-Shrink (GS) [40], the Incremental Association (IAMB) [41], the Fast Incremental Association (Fast-IAMB) [42], and the Interleaved Incremental Association (Inter-IAMB) [41]. In score-based learning, a network is learned from the network's best goodness of fit by assigning a network score from the application of a general heuristic optimization technique to each candidate network. A commonly-used example of a score-based learning algorithm, for example, Hill-Climbing (HC), learns a network structure using a step progress process. In HC learning, a graphical score is computed for a randomly assigned network structure as a network score at the beginning of the process. A new score is computed from the assigned network structure by adding, deleting, or reversing an arc's direction one at a time. The new graphical score will become the network score if it has a higher value than the previous one. The process of the computation repeats again and again until the network score reaches to its maximum. The corresponding network structure, which has the maximum network score, has the best goodness of fit to the network data. HC is chosen as the algorithm learning approach in this study because of its flexibility and power to handle the hybrid data types existing in our network data. To enhance the robustness of the network structure generated from score-based causal relationships between child and parents sets, a bootstrap sampling technique with an iteration of 5000 is performed, and two criteria—conditional dependence strength of above 80% and arc directions appearing in more than 50% of the iterations—are applied to the HC structure learning.

The first disease infection likely occurs between the end of June and July, which is during the flowering stage of the grape (Figure 3). Establishing the initial modeling date is important because this can influence the model accuracy of disease risk. Modeling results were examined for four selected starting dates to determine the best date for initial disease risk modeling. These dates were selected under different assumptions: (1) the flowering date as the time of primary infection onset; (2) the mid-flowering date as the likely onset of secondary infection; (3) July 1st when the infection spreads to other plants, and (4) using the actual observed date of infection start as the estimated model start date may improve disease risk predictions. At the beginning of each growing season (1 April), the timing of the grapevine growing and mid-flowering stages were also estimated by the CGDD index (Equation (1)) using daily mean temperature. The estimation of the PM growth factor is based on selected dates using Equations presented in Section 2.4 and are specified for both the supervised and algorithm learning.

Table 2 summarizes the random variables used for network learning, including the additional considered day-to-day variability of relative humidity. Bayesian network modeling in both supervised and algorithm modes are trained for the three susceptible grape cultivars using observational data from 2000 to 2010 and then tested against actual pathogen occurrence and progression in 2011. Model forecast accuracy was evaluated comparing supervised and algorithm learning and a range of starting dates. The best-performing model was then used to examine the forecast performance and optimal forecast window length using GEFS input data.

Table 2. Variables for structural learning by the Grape PM model.

Parameters	Descriptions	Data Type
DI	Disease incidence	Continuous
DI_P	Recent disease incidence before a latent period	Continuous
DR	Dispersal rate	Continuous
LP	Number of latent period are done at current day	Discrete
PIR	Primary infection rate	Continuous
$P_{maxacc3}$	Degree-Days based risk assessment model (3 °C)	Continuous
RH	Relative humidity	Continuous
PS	Plant stage	Discrete
SIR	Secondary infection rate	Continuous
Type	Susceptible cultivar type	Discrete
T_{mean}	Daily mean temperature	Continuous
TP	Daily total precipitation	Continuous
WS	Wind speed	Continuous

3.2. Forecast Skill under Different Learning Modes

The performance of the forecast model under supervised and algorithm learning was evaluated and inter-compared using: (1) model skill in goodness-of-fit testing, which examined how well the model worked in accurately reproducing training data; and (2) model performance in prediction, providing benchmark information about model accuracy using forecast weather data. The learned model structure identified a subset of random variables listed in Table 2. Random variables in a subset were selected by removing one or more unclear but considerable factors: the degree-days based assessment model (Pmaxacc), relative humidity (RH), and plant stages (PS) one at a time from the full data. A total of eight cases were examined: Case 1, full data; Case 2, remove RH; Case 3, remove PS; Case 4, remove Pmaxacc; Case 5, remove PS and RH; Case 6, remove RH and Pmaxacc; Case 7, remove PS and Pmaxacc; and Case 8, remove PS, Pmaxacc, and RH. Over-learning or over-fitting is a common problem in parameter learning, in which the network model is forced to accommodate data or parameters that do not contribute information; this results in degraded model predictive skill. *k*-fold cross-validation, where *k* is the number of years in the training data, has been applied to prevent over-learning. In this approach mean-absolute-error (MAE) and root-mean-squared-error (RMSE) are used as metrics to identify prediction bias and for variance comparison. Metrics used for model skill comparison for prediction results similarly include the MAE and RMSE generated for the 2011 growing season.

Cross-validation using the *k*-fold method is a re-sampling technique often used to evaluate the prediction performance of a machine learning model using limited data sample as training data. In *k*-fold cross-validation, the training data are split into *k* subsets of equal size which are used to assess how the omission of one subset affects the learning of a Bayesian network from the rest of the subsets, by generating model predictions for the omitted subset. In this study, the training data set were split into k subsets by years. A single year is randomly removed to act as testing data, and the rest of the data are used for parameter learning using both supervised and algorithm learning approaches. The corresponding results of bias (MAE) and variance (RMSE) loss functions can be applied to measure

deviation and discrepancy, separately, to determine how close model predictions were to the actual outcomes. Both MAE and RMSE can be defines as:

$$MAE = \frac{1}{n}\sum_{i=1}^{n}|y^{(i)} - \hat{y}^{(i)}| \tag{14}$$

$$RMSE = \sqrt{\frac{1}{n}\sum_{i=1}^{n}(y^{(i)} - \hat{y}^{(i)})^2} \tag{15}$$

where $(y^{(i)}) - \hat{y}^{(i)}$ is the residual or error between the model predictions and the actual values. A lower value of MAE and RMSE indicates a model exhibiting better performance.

4. Model Forecast Evaluation

Sensitivity analysis (i.e., for a static or time-independent model) involves varying input variables, typically one at a time, to measure how it impacts a model's output. Scenario analysis involves varying input variables to measure its impact on a future value either as future model predictions (if internally forced), or as projections (if externally forced). In the context of dynamic or time-dependent (i.e., forecast) models, shifting an input (e.g., climate or weather input variable) that is time-dependent generates variation over time. Furthermore, when forecast models have cumulative variables or interactions between multiple variables, future model outcomes can also become dependent and coupled across time. In such cases, sensitivity and scenario analysis becomes more integrated and less independently defined.

To understand the effect of a warmer and colder climate on DI model forecasts for the three northern cultivars, we varied the input daily mean temperature by 2 °C in 2011. The runs with warmer and colder temperature were referred to as warm and cold year scenarios, respectively, and compared to the actual or baseline temperature at the study site in 2011. We also varied the model's forecasting window length from 1, out to 16 days, to assess how robust the model's forecasts of DI are over time, how sensitive its error is to the length of the forecasting window, and evaluate the GEFS reforecasted weather data as a model input for generating forecasts out to 16 days in advance. This analysis involved comparing the model's forecast error statistics (MAE and RMSE) over time (days). The Bayesian network model with supervised learning, was used with GEFS reforecasted weather data for climate/weather variable input. Starting 1 April 2011, host plant stages were estimated using historical weather data and used to identify the mid-flowering date (2 July) to initiate the forecast model. Canopy-height daily maximum/minimum temperature, total precipitation, air pressure, specific humidity, and U/V component of wind were selected. Scalar mean daily wind speed was computed using the U/V-component wind variables. The daily mean temperature was calculated as the mean of the daily maximum and minimum temperature. The relative humidity was calculated from specific humidity using daily mean temperature and air pressure as inputs to the statistical R programming function $SH2RH$ from the "humidity R package". Weather data was averaged from 11 ensembles and used as model inputs for DI forecasting at a 16-day window. For each day after 2 July, the calibration of the Bayesian network model was performed using historical data from 1 April up to the present day and used for DI forecasting using data generated from GEFS.

5. Model-Based Fungicide Spray Program

A fungicide spray program was identified for maximizing spray efficiency for disease control based on the Bayesian network model and forecasting windows (refer to Sections 3.2 and 4). The program guides grape advisor or growers by providing the best times to spray fungicide for PM control in relation to disease risk (future disease incidence), local weather, and regional climate variability.

An optimal model-based fungicide spray program was generated under the following assumptions: (1) The rate of disease incidence given application of fungicide spray follows an exponential decay function of the form $A = A_0 * \exp(kt)$, where A_0, A, k, and t are the disease incidence at the current day, initial disease incidence, decay rate of disease incidence, and time in days, respectively; (2) fungicide spray is washed off when cumulative precipitation reaches 25 mm or more from the date of spray application. The decay rate of fungicide spray efficiency remaining as a function of precipitation amount was simply estimated using a linear function of $y = -0.04 * p$, where y is the fungicide "effectiveness rate" under precipitation and takes a value between $[0, 1]$. p is the cumulative total precipitation and takes values from $[0, 25]$, with $p = 25$ if cumulative precipitation exceeds 25 mm; and (3) The occurrence of precipitation events is independent of fungicide application events. That is, the occurrence of precipitation is not affected by fungicide spraying. By setting the amount by which an application of fungicide can reduce the incidence of powdery mildew from $A_0 = 20\%$ to $A = 8\%$ for 10 continuous days with no rain $t = 10$. We generate the value for $k = -0.0916$ and the equation used to estimate the disease incidence under fungicide spray control influenced by the uncertainty of precipitation is:

$$A(t) = A_0 * (1 - (1 - \exp(-0.0916t) * (1 - 0.04p)) \quad (16)$$

where $A(t)$ is the disease incidence after t days of fungicide spray. A_0 is the DI on the fungicide spray day. A disease incidence profile was then generated for fungicide spray using forecast disease incidence and Equation (16).

6. Results

The performance of the forecast model was evaluated by varying the starting date (i.e., 4 selected starting dates) using a subset of variables (Table 3). After determining the best model starting date (i.e., first disease date) simulation runs using 8 different variable subsets were performed (Table 4). These tables provide a summary of the resulting mean-absolute-error (MAE) and root-mean-squared-error (RMSE) validation metrics for the northern grape cultivars. The forecast model was trained using data from 2000–2010 and validated using data for 2011.

Model forecast skill was evaluated based on *k*-fold validation statistics (MAE, RMSE) across the years 2000–2011 which removes *k* years at a time from the data and re-assesses forecast skill. The model was also validated by training the model on all of the historical data (2000–2010) (i.e., removing only data for year 2011) and then comparing its forecasts against 2011 data. Smaller values in both MAE and RMSE indicate higher forecast skill.

For supervised learning, the optimal initial date for start disease risk prediction was starting from first disease date in Case 1, containing all the network variables in the modeling structure. This run had the smallest values of cross-validated RMSE and predictive error in 2011 (MAE and RMSE). The smallest value of MAE (1.83) for training data was in Case 6 with model initialed from the flowering date but with higher values in RMSE for training data and MAE and RMSE for prediction data in the first disease date. The highest values of MAE and RMSE in both training and prediction data were from Mid-Flowering data with Case 6, which do not include relative humidity and degree-days based risk assessment model in the model structure.

In algorithm learning, Cases 2 and 3 performed the best, which did not contain relative humidity or plant stage. The best model performance was from the first disease date in Case 2 that had the smallest values of MAE and RMSE in both cross-validation and prediction. The highest values of cross-validated MAE (3.9) and RMSE (6.13) were for flowering date in Case 2, which had small MAE (0.57) and RMSE (0.99), as with the first disease date. The highest MAE and RMSE values in prediction was for flowering, which had high values of MAE and RMSE similar to mid-flowering. In general, cross-validated MAE and RMSE values were higher than the prediction values of these metrics in historical drought years of 2000, 2002, and 2008. Model accuracy of disease prediction was also evaluated with and without drought conditions, by adding a binary factor identifying historical years of drought (2000, 2002, 2008). The best performing model for supervised learning with drought years

factor being Case 3 with model initialed from the first disease date, which has MAE and RMSE of 2.36 and 4.16 from training data and 1.13 and 1.52 from predictions, respectively. The best performing network structure in algorithm learning being Case 2 from the first disease date which has smallest values in MAE and RMSE from both training and prediction data than other selected dates. For both supervised and algorithmic learning, the model without drought had smaller values of MAE and RMSE than those for drought years.

Model performance under structural learning for the 8 network variable sets from the first disease date are shown in Table 4. We describe these specific cases here below in greater detail. In supervised learning, the smallest values of MAE and RMSE were from Cases 1 and 2, which contains plant stage and the degree-days risk assessment submodel. MAE and RMSE were higher when the model structure does not contain plant stage (Cases 3 and 5) or degree-days risk assessment model (Cases 4 and 6) and was at the highest values when model structures (Case 7 and 8) did not contain both plant stage and degree-days risk assessment model. It has been noted that network structures in algorithm learning are learned based on network scores from an algorithm; a child was linked only by the parents with significant influences. A child can have the same network structures from two sets of network random variables, with both contain the same parents with significant influences. In algorithm learning, the best performing network model is Cases 1 and 2 with MAE (2.11) and RMSE (3.69) from cross-validation and MAE (0.56) and RMSE (0.87) from model prediction. There was no local distribution learned for disease prediction when the plant stage has removed from network variables (Cases 3 and 5). While network variable does not contain both plant stage and degree-days assessment model (Cases 7 and 8), MAE and RMSE were three times higher for training data (MAE 6.88 and RMSE 9.59) and more than ten times higher for prediction (MAE 5.21 and RMSE 7.34) than Cases 1 and 2. When comparing the best model results between supervised and algorithm learning, supervised learning gained smaller values in MAE and RMSE from the training data from 2000 to 2011 with prediction MAE and RMSE in 2011 slightly higher than from algorithm learning.

Table 3. Inter-comparison of model performance in parameter learning from both supervised and algorithmic learning in a total of 32 subsets of network random variables in four different model starting dates. The table shows the best model results of the network random variables and model start date. In addition, a binary factor of drought years (1 as in 2000, 2002, and 2008; 0 as in the rest of study years) was added as a parent to disease incidence to examine the model performance of disease incidence predictions in the hot years. Model performance was compared using mean-absolute-error (MAE) and root-mean-square-error (RMSE) from *k*-fold cross-validation, and model prediction skills in predicting disease incidence using observed climate variables in 2011. Smaller and non-negative values in both MAE and RMSE indicate higher model performance.

		Supervised					**Algorithmic**			
		Cross Validation		**Prediction**			**Cross Validation**		**Prediction**	
Without Drought	**Data Case**	**MAE**	**RMSE**	**MAE**	**RMSE**	**Data Case**	**MAE**	**RMSE**	**MAE**	**RMSE**
Flowering	6	1.83	3.71	1.45	2.65	3	3.31	5.46	2.03	2.7
Mid-Flowering	6	2.44	4.33	1.87	3.03	2	3.9	6.13	0.57	0.99
July 1st	1	2.13	3.82	1.4	2.27	3	3.51	5.36	0.95	1.37
First Disease Date	1	1.86	3.23	0.99	1.57	2	2.11	3.69	0.56	0.87
		Supervised					**Algorithmic**			
		Cross Validation		**Prediction**			**Cross Validation**		**Prediction**	
Without Drought	**Data Case**	**MAE**	**RMSE**	**MAE**	**RMSE**	**Data Case**	**MAE**	**RMSE**	**MAE**	**RMSE**
Flowering	4	2.24	4.65	1.33	2.5	3	3.9	6.6	2.03	2.7
Mid-Flowering	4	2.93	5.41	1.71	2.83	2	4.32	7.78	0.58	0.99
July 1st	4	2.57	4.94	1.66	2.8	5	3.92	6.2	1.04	1.48
First Disease Date	3	2.36	4.16	1.13	1.52	2	2.64	5.09	0.55	0.86

Table 4. Comparison of model performance of parameter learning starting from the first disease date for 8 subsets of network random variables. Forecast skill (MAE and RMSE) from *k*-fold cross-validation is listed. Smaller and non-negative values in both MAE and RMSE indicate higher model performance. The dash "-" indicates there is no available model for forecasting DI using the selected network random variables.

	Supervised				Algorithmic			
	Validation (2000–10)		2011 Forecast		Validation (2000–10)		2011 Forecast	
Case	MAE	RMSE	MAE	RMSE	MAE	RMSE	MAE	RMSE
1	1.86	3.23	0.99	1.57	2.11	3.69	0.56	0.87
2	1.86	3.24	0.99	1.55	2.11	3.69	0.56	0.87
3	2.22	3.52	1.46	2.02	-	-	-	-
4	2.25	4.12	1.82	2.96	4.2	6.83	2.43	4.09
5	2.23	3.52	1.43	2.01	-	-	-	-
6	2.24	4.1	1.81	2.94	4.2	6.83	2.43	4.09
7	3.75	6.48	3.08	5.98	6.88	9.59	5.21	7.34
8	3.74	6.48	3.1	6.04	6.88	9.59	5.21	7.34

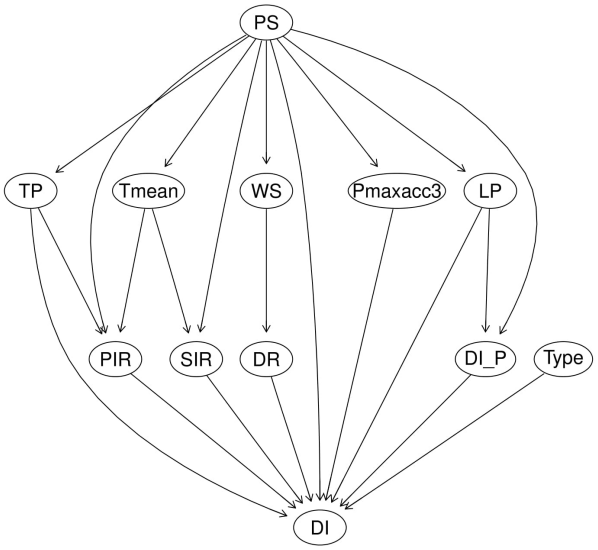

Figure 6. Directed acyclic graphical (DAG) representation of Bayesian network model structure identified by supervised learning of grape PM. The causal relationships between the variable were linked by existing empirical and published scientific peer-reviewed knowledge on the interactions between the climate, host, and pathogen. Variables in the DAG representation includes: plant stage (PS), total precipitation (TP), daily mean temperature (Tmean), wind speed (WS), degree-days based risk assessment model $P_{maxacc3}$ (3 °C), latent period (LP), primary infection rate (PIR), secondary infection rate (SIR), dispersal rate (DR), recent disease incidence (DI_P), cultivar (Type), and disease incidence (DI).

The representative DAG for the best-performing model under supervised (Case 2) and algorithm (Case 2) learning is shown in Figures 6 and 7. In the case of supervised learning, the DAG is a plant stage based network. This network structure assumes: (1) the susceptibility of the grapevine to the PM development is influenced by changing weather and climate that varies by plant stage, (2) DI is independently affected by a set of factors including: precipitation (TP), primary infection rate (PIR), secondary infection rate (SIR), wind-speed (WS) influenced dispersal rate (DR), plant stage (PS), the degree-days based disease risk assessment model ($P_{maxxacc3}$), latent period (LP), past DI (DI_P); and genes cultivar types (Type). The network structure learned from supervised learning shows causal relationships based on existing knowledge, with dispersal rate (DR) of grape PM spores being influenced by wind-speed conditions, secondary infection (SIR), and temperature (Figure 6).

In algorithmic learning, causal relationships were generated from the independent random variables to maximum the network score of a network structure from bootstrap sampling technique with strength above 0.8 and direction above 0.5 from 5000 interactions. The learned model structure and linkages between variables from algorithmic learning (Figure 7) shows DR not linked to DI as it was not identified as a significantly strong predictor. This suggests that DR needs to be better represented and that the current DR equation does not represent the observed PM epidemic. Significant correlations between grape cultivar types, plant stage (PS), and the risk assessment model ($P_{maxacc3}$) with DI was detected from the algorithmic learning.

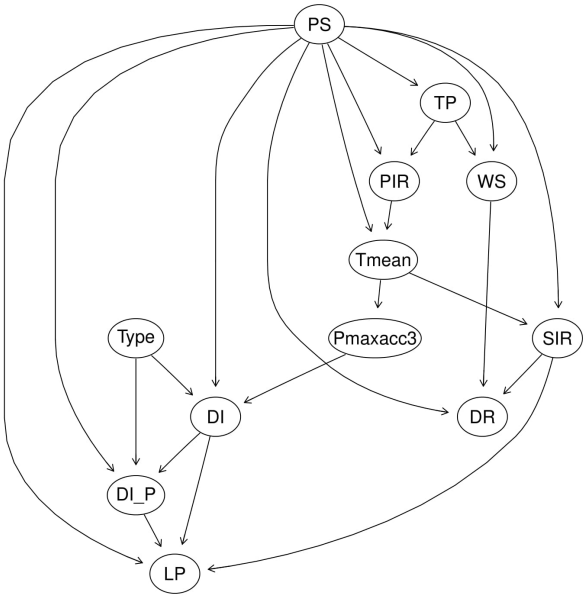

Figure 7. DAG representation of Bayesian network model structure learned by algorithmic learning. The structure was learned from bootstrap sampling technique under 5000 iterations with arc strength above 0.8 and arc direction above 0.5. Variables learned in this Bayesian network are a combination of observed climate variables and the estimated development factors of grapevine and the pathogen of grape PM. Variables in the DAG representation include: plant stage (PS), total precipitation (TP), daily mean temperature (Tmean), wind speed (WS), degree-days based risk assessment model $P_{maxacc3}$ (3 °C), latent period (LP), primary infection rate (PIR), secondary infection rate (SIR), dispersal rate (DR), recent disease incidence (DI_P), cultivar (Type), and disease incidence (DI).

The performance of the forecast model under supervised and algorithmic learning for the three northern grape cultivars for training (2000–2010), and prediction in 2011, is shown in Figure 8. Both supervised and algorithm learning have similar model performance (both in MAE and RMSE). Model accuracy was high in the recorded drought years of 2000, 2002, and 2008 with values of MAE and RMSE were varying from 3 to 5 and from 4 to 7, respectively. The model performance worked well in non-drought years with MAE and RMSE were varying around from 0.56 to 2.6 and from 0.86 to 3.7, respectively. Model performance in both supervised and algorithm learning tended to be more and more accurate (smaller values in MAE and RMSE) in disease prediction in drought and non-drought years as the Bayesian network model has learned from more and more reliable input data. Disease performance in algorithm learning tends to be more sensitive in climate-related disease predictions than in supervised learning with MAE and RMSE in algorithm learning were higher than in supervised learning in drought years and smaller in non-drought years. The smallest value of MAE 0.99 and 0.56 in supervised and algorithm learning, respectively, found in 2011. The smallest value of RMSE 1.57 in supervised learning found in 2010 and 0.87 in algorithm learning found in 2011.

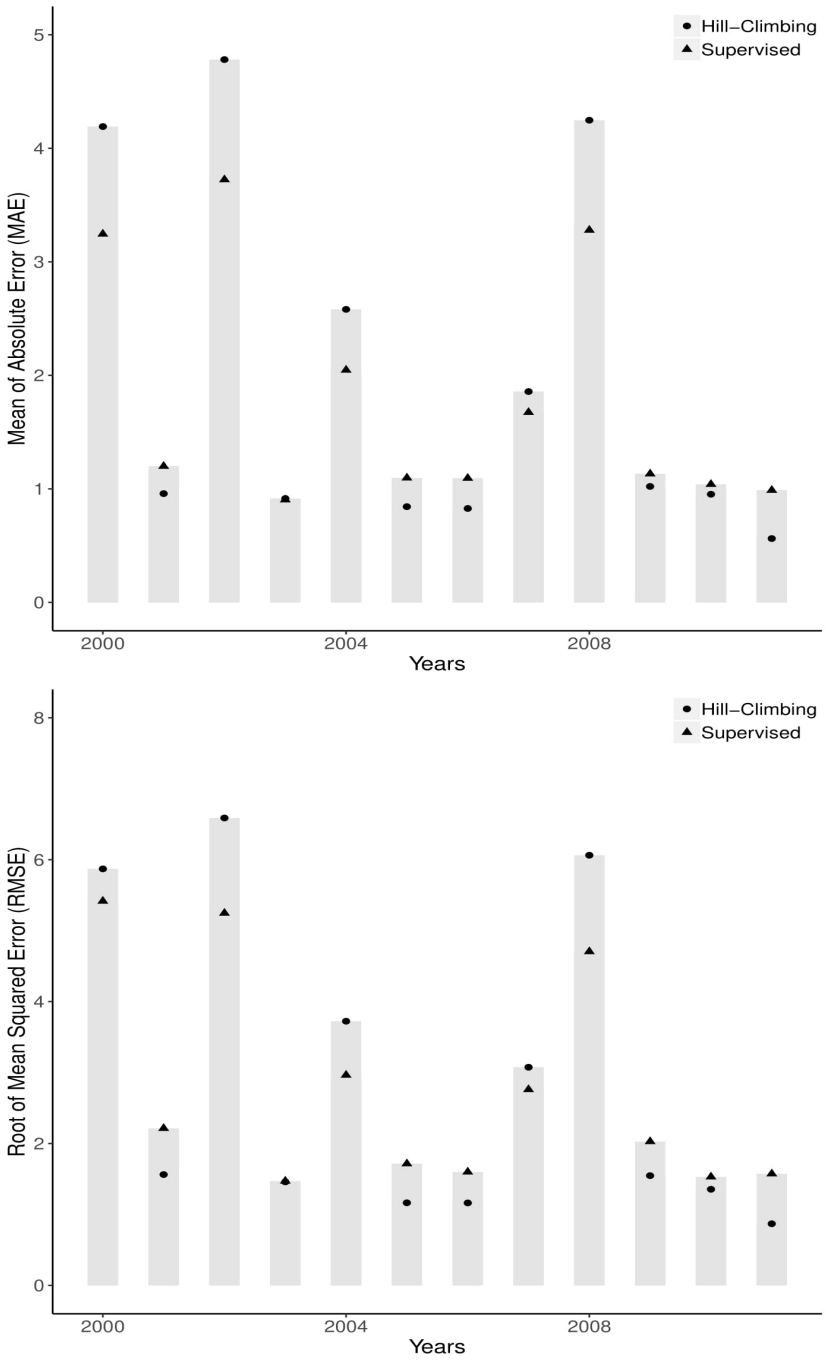

Figure 8. Model forecast skill from *k*-fold cross-validation (2000–2010) and 2011 year validation in both supervised (circle) and hill-climbing based algorithmic learning (triangle). MAE and RMSE were computed for the three susceptible grape cultivars in the testing year. Smaller values in both MAE and RMSE indicates higher forecast skill.

Model predictions of grape PM for the three cultivars from both supervised learning in Case 2 (dotted line) and algorithmic learning in Case 2 (dashed line) across the three plant stages of flowering, setting, and veraison are shown in Figure 9. The predictions are shown compared to observed DI in 2011 (solid line). DI of conidial infection generally starts from the end of June until the end of the growing season. For Geisenheim-318 and Frontenac, the Bayesian network in both supervised and algorithm learning did work well in predicting disease incidence in 2011 with supervised learning has slightly better performance the hill-climbing-based algorithm learning in predicting DI over the growing season. Overall, the best model is Case 2 with supervised learning for which the model has

learned using existing knowledge about disease development of grape PM using the full set of random variables but without relative humidity (as listed in Table 2).

Forecast evaluation plots of DI in warm (dotted line) and cold (dashed line) years for the three cultivars: Chancellor (top), Geisenheim-318 (middle), and Frontenac (bottom) in 2011 by increasing and decreasing daily temperature in 2001 by 2 °C are shown in Figure 10. The three grape cultivars have a similar response to the changing temperature but differ in the susceptibility to grape PM. In the warm year, DI tended to be higher than the normal for most of the growing seasons except in mid-August. The maximum DI over the growing season was higher in warm year than in the normal. while in the cold year, model prediction of DI has tended to lower than the normal except the beginning of August.

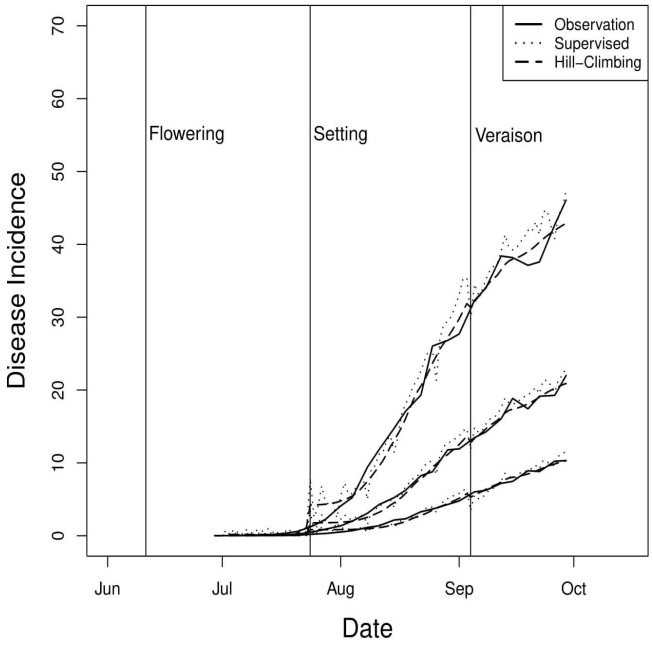

Figure 9. Model predictions of DI of PM for the three grape cultivars: High susceptible Chancellor (top), Medium susceptible Geisenheim-318 (middle), and the low susceptible Frontenac (bottom) in 2011. Model predictions from both supervised (dotted line) and algorithm (dashed line) learned Bayesian network are shown alongside the observed daily DI. The three vertical lines from left to right are the estimated plant stage of grapevine: flowering, setting, and veraison stages. DI of grape PM in 2011 started from 29 June until the end of the growing season.

Evaluation of the optimal forecasting window for DI prediction of grape PM using the up to 16 days high-performance forecast data in GEFS is shown in Figure 11. Averaged MAE and RMSE were calculated by taking the average of MAE and RMSE, separately, computed from the model predictions and actual disease incidence in different forecast windows. Lower values of MAE and RMSE indicate lower model uncertainty and higher model forecasting skill. The smallest values of averaged MAE were for 6 days forecasting (0.846), and the most significant values was for 16 days forecasting (0.926). Averaged MAE tended to decreased from 0.863 to the minimum values of 0.846 when forecasting windows changes from 1 to 6 days and increased to the maximum values of 0.926 when forecasting windows changes to 16 days. For averaged RSME, the smallest values were for one-day forecasting (1.029) and tended to the maximum values (1.344) when forecasting windows changed from 1 to 16 days. Overall, both averaged MAE and RMSE in up to 16 days forecasting windows were considerably small, our fungicide spray program was developed using the disease incidence predictions and climate variables from the GEFS in 16 days forecasting window.

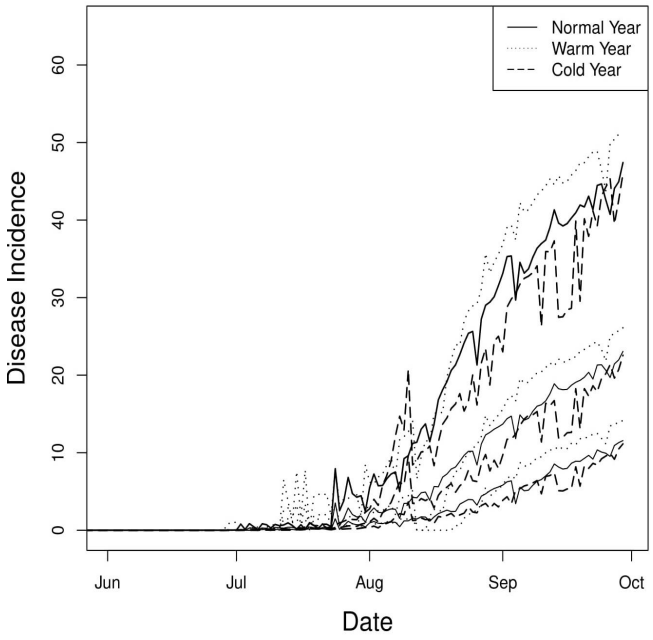

Figure 10. Sensitivity analysis of model predicted DI for Chancellor (top), Geisenheim-318 (middle), and Frontenac (bottom) cultivars, by changing temperature by 2 °C (warm and cold year scenarios). Daily temperature in 2011 is shown as a reference baseline (solid line).

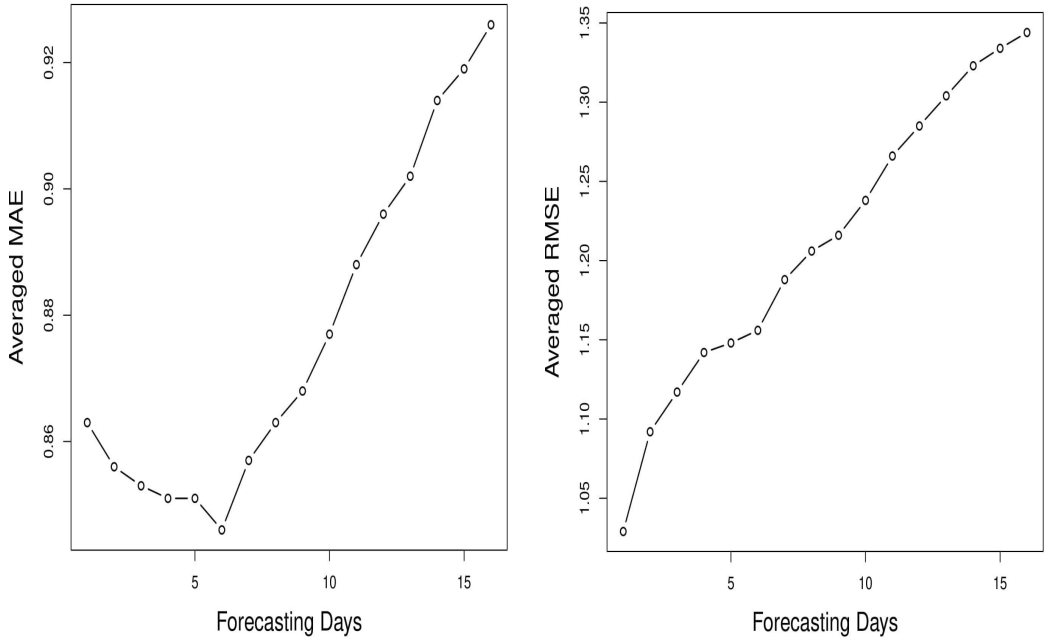

Figure 11. Sensitivity of DI prediction error to forecast window size (1–16 days), measured using average MAE and RMSE, under supervised learning and GEFS climate input.

We further compared our fungicide spray program to two existing benchmark programs, the UC-Davis, and the degree-days (with a 6 °C base temperature) based risk assessment model. The UC-Davis program is a score based program to provide suggestions for fungicide spray in different spray schedules. The UC score is a daily temperature-based model, which the model initials from the day of the first primary infection. The UC-Davis program applies fungicide spray with an interval of 14 to 21 days, if the UC score is less or equals to 30; a 10 to 17 days interval, if the

UC score is from 40 to 50; or a 7-days interval, if the UC score is above 60. The degree-days based risk assessment model specified a spray schedule interval of 7 to 14 days, if $P_{maxacc6}$ is above 1% in Chancellor and Geisenheim-318, and 0.5%, for Frontenac. Figure 12 represents the application of the UC-Davis program and the degree-days based risk assessment model for disease control of grape PM at the experimental farm in Quebec in 2011. Fungicide spray applications from the UC-Davis exhibited a case of over-spraying in relation to the actual disease severity for each of the three cultivars. The UC scores were above 60 from 9 July until 18 September and suggests a high frequency of fungicide sprays. The degree-days based risk assessment model provided better disease control than the UC-Davis model by reducing the number of scheduled fungicide spray. This program suggested initial fungicide spray starts on 7 August for Chancellor, 10 August for Geisenheim-318, and 12 August for Frontenac.

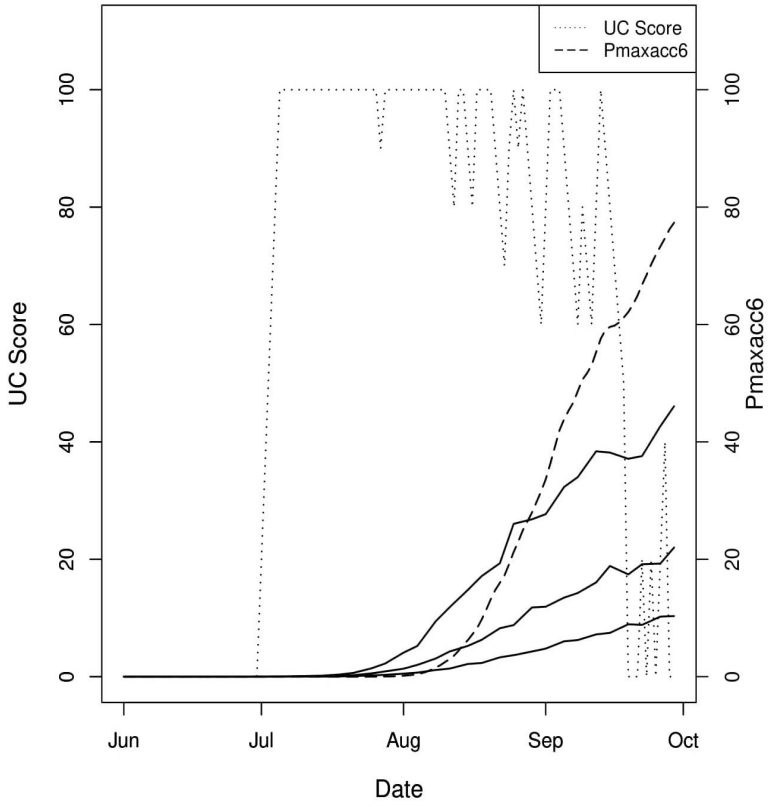

Figure 12. Fungicide spray programs of the UC-Davis and the degree-days risk assessment model to grape PM in 2011. The dotted line indicates the threshold-based UC score from the UC-Davis model. The long dashed line indicates the schedule-based model scores from the degree-day model. The solid line indicates the DI of Chancellor (top); Geisenheim-318 (middle); and Frontenac (bottom).

The model-based fungicide spray program provides a spray strategy up to 6 days in advance and forecasts disease risk with a lead time of up to 10 days to optimize the efficiency of fungicide spray under the uncertainty of precipitation. An example of such a model-based fungicide spray program is for the date of 27 August, when a high rainfall event was forecast to occur on August 29 and 30 with precipitation of 46.46 mm and 121.129 mm, respectively (Table 5). The table shows the average DI from 10 days of disease control under 6 different fungicide spray dates (28 August–2 September) for the three susceptible cultivars. The best spray day for the three grape cultivars was 1 September having an average DI of 22.72 for Chancellor, 9.47 for Geisenheim-318, and 3.82 for Frontenac. Figure 13 shows 3D plots of 10-day daily DI for Chancellor (top-left), Geisenheim-318 (top-right), and Frontenac (bottom left) for the six different spray days, from a low to high level of disease severity. The 2D plot (bottom-right) shows the forecast daily DI for Chancellor (dotted line), Geisenheim-318 (dot-dashed line), and Frontenac (dashed line) on the optimal spray day.

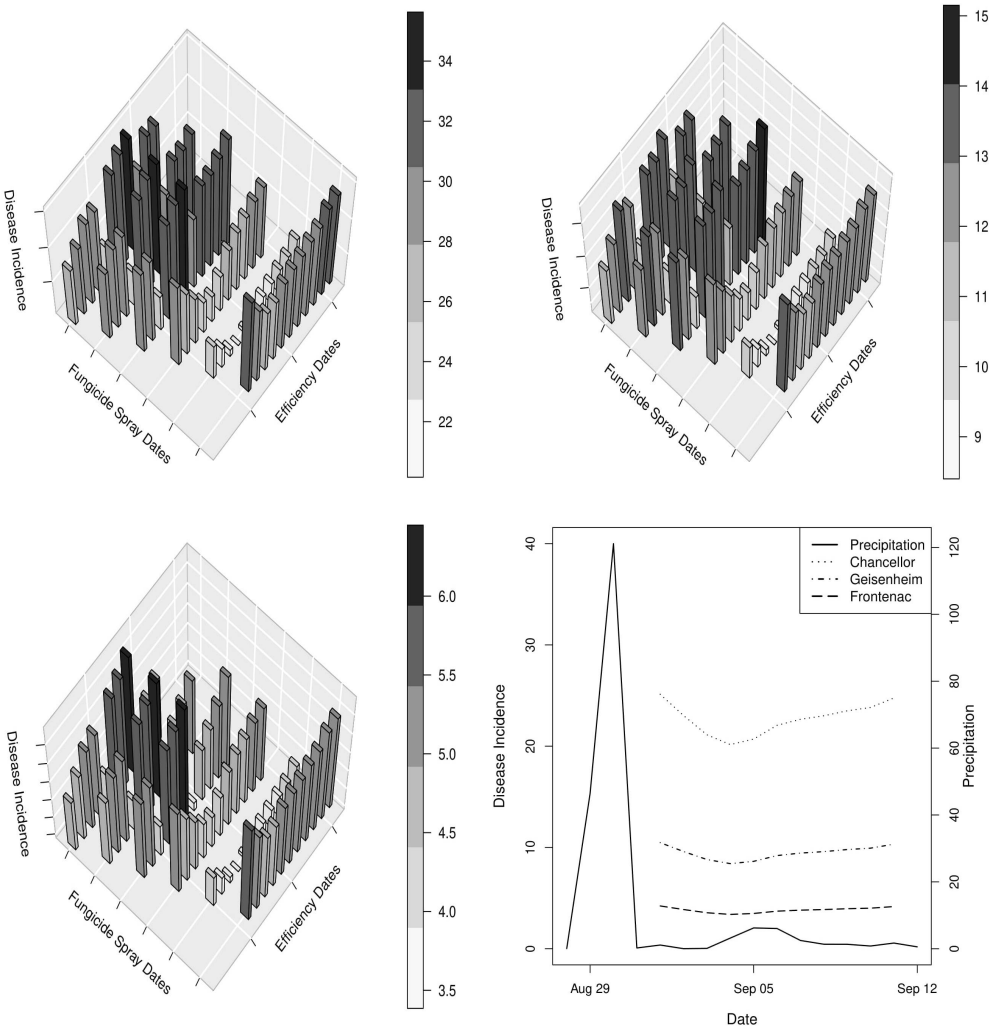

Figure 13. 3D plot of the fungicide spray strategies of Chancellor (upper-left), Geisenheim-318 (upper-right), and Frontenac (lower-center) from the forecast model on 27 August 2011 for six fungicide spray dates and corresponding 10-day DI based on the 16-day Global Ensemble Forecast System (GEFS) reforecast climate input. (Lower-right) 2D plot of the 10-day daily DI of the optimal spray date for Chancellor (dotted line); Geisenheim-318 (dot-dash line); and Frontenac (long-dash line) based on DI on 27 August 2011 and 16-day GEFS input. The solid line indicated the daily cumulative total precipitation from GEFS on 28 August 2011. Note: Darker color indicates higher disease severity.

Table 5. DI values for the forecast model-based fungicide spray program on 27 August 2011.

Fungicide Spray Date	Chancellor	Geisenheim-318	Frontenac
28 August	31.59	13.27	5.21
29 August	32.09	13.52	5.26
30 August	32.55	13.74	5.32
31 August	27.91	11.92	4.94
1 September	22.72	9.47	3.82
2 September	31.04	13	5.5

7. Discussion

The best performing model for grape PM disease risk forecasting at the experimental farm in Quebec was Case 2 with model structure learned using supervised learning. Figure 6 shows the learned structure found for this model. DI for the three cultivars was relatively consistent with the degree-days risk assessment model having a 3 °C base temperature and plant stage, but not with relative humidity included. Instead, the best local distribution of the causal relationship of DI involved total precipitation, primary infection rate, secondary infection rate, dispersal rate, plant stage, risk assessment model, latent period, and vary in susceptible cultivar type. Figure 9 shows that the supervised Bayesian network has a very high performance in disease risk forecasting for the three susceptible cultivars over the plant stage that are affected by PM disease.

Model validation of DI shown in Figure 9 shows the resultant model network structure from both supervised and algorithm learning. Supervised learning had a slightly better performance in predicting DI of grape PM over 2000–2011. Smaller values of MAE and RMSE in non-drought years than in drought years (i.e., 2000, 2002, 2008) indicates that the model has better forecasting skill in non-drought years, and the complex climate conditions significantly influence the development of DI in drought years, summarized in Table 3. The development of PM in drought years was not well explained by the use of a simple binary factor suggesting that a more complex model of DI involving autocorrelation across multiple years (i.e., not just a single year factor) may be needed. The comparison result of the four selected model starting dates indicates the best time to initiate the modeling of disease incidence is when the disease occurs on the farm.

Model forecast evaluation results are shown in Figure 10, whereby the three cultivars have a similar response to the changing temperature. There is a significant difference in DI between the normal year and the warm and cold years, which by adding or dropping the daily temperature by 2 °C, separately. DI tends to be more severe in warm years and less severe in cold years when compared to the DI in the normal year, which explains the complex interactions between the development of the pathogen of powdery mildew and its host under the influences of heat stress conditions. The warm temperature at the beginning of the growing season advances the bud break of the host as well as the development of ascospores from over-wintered cleistothecia. Then dispersal and infection, caused higher than normal DI.

The sensitivity analysis of model prediction of grape PM for the three cultivars in 2011 using the 16 days climate variable from GEFS shown in Figure 11 indicates the GEFS data has very high performance in predicting DI in Quebec. Although the averaged MAE varied from 0.863 to 0.926 and averaged RMSE varied from 1.029 to 1.344 when forecasting window changes from day 1 to day 16, both averaged MAE and RMSE are all small (less than one percentage in averaged MAE and 1.5 percentage in averaged RMSE). The UC-Davis fungicide spray program shown in Figure 12 shows an over-estimate of DI of PM of most of the growing season, results from over-spray suggestions of scheduled fungicide spray application in disease control.

The degree-days based risk assessment model provides better suggestions for disease control than the UC-Davis by delaying the initiation of the fungicide spray program for disease control. However, it does not consider the difference in susceptibility of cultivars. Our fungicide spray program was developed from the best-performing Bayesian network forecast model with supervised learning out to 16 days guided by GEFS reforecast climate. This program provides fungicide spray suggestions up to 6 spray day strategies with 10-days disease control forecasting by using information about forecast DI and the efficiency of fungicide spray under uncertainty climate changes (precipitations). An example of this is presented for 17 August 2011. This example data was selected because there are two significant forecast rainfall events on 29 August (46.46 mm) and 30 August (121.129 mm) and a few small rainfalls from 31 August–12 September. Table 5 shows the best spray day for the three susceptible cultivars is on September 1st with results average DI of 22.72, 9.47, 3.82 for Chancellor, Geisenheim-318, and Frontenac, respectively, in 10 days after the spray has applied. The 3D plot in Figure 13 shows model forecasts of DI extending out to 10 days in the future for the different spray

days. The 2D plot shows the daily DI based on a current day for fungicide spray under variation to changing precipitation. With these forecast curves or foresight information output from the forecast model, grape producers can make a better decision about the best timing to apply fungicide spray for different grape cultivars in order to maximize the spray efficiency and to protect grapevines over the growing season.

8. Conclusions

Grape PM is one of the most common diseases responsible for significant reduction in grape yield in North America. The rate of development and epidemiology of this disease are influenced by regional-scale, longer-term climate and localized, shorter-term weather uncertainty. It also varies with growth stage and the genetics of a grape cultivar, making it difficult to develop efficient strategies for disease management. Most research on epidemiology and modeling of PM has been conducted for temperate climates. In this study, using 13 years of data, we developed and tested a novel Bayesian network model to forecast disease risk (i.e., the development of DI of conidial infection in grape PM on leaves) for three susceptible cultivars calibrated to site-specific data obtained from an experimental vineyard in Quebec. The forecast model generates high prediction (based on in-sample validation testing) also out to 16 days ahead using GEFS, and enables a reliable fungicide strategy for disease control with a 6-days forecasting window. Fully-independent validation data is needed to evaluate how well our model can forecast grape PM disease in other vineyards with differing grape cultivars, cultural practices, and environmental conditions.

There is observed uncertainty in DI that is not fully explained by our current model. Our modeling focuses on leaf PM epidemic and resistance at a time when the grape cluster is most susceptible to the presence of PM, whereby leaf infection is usually the first warning and signal to the vines treatment and leaf protection is a limiting factor to grape yield. Nonetheless, relying solely on leaf resistance is a current shortcoming of the forecast model. An operational protection model would need to consider leaves and grape berry clusters. This would require extending the current model to be spatially-explicit, because berry clusters are sufficiently complex in terms of their development and exhibit susceptibility that is spatially heterogeneous within vineyards and strongly dependent on phenological age [27]. Recent spatial model simulations of fungicide use show that applying a fungicide early at flowering may significantly reduce PM diseased area, by up to 81% at the end of the season by delaying the epidemic onset. It also helps to maintain a low level of disease and to minimize potential PM dispersion from leaves to bunches [43]. Burie et al. (2011) demonstrate the strong dependence of PM disease progression on grapevine growth rate (vigor) and regional climate using a multi-scale dynamic grapevine-PM model [44]. Future work stemming from the current study will require spatio-temporal vineyard data and additional data from other measurement variables such as: canopy leaf wetness, fungicide type, and efficiency, spatial locations of susceptible grape cultivars, and berries infection, yield loss.

The developed model-based fungicide spray program provides an improved way to minimize the total number of sprays and their timing for optimizing grape PM spray efficiency and its recommendations could, in the future, be used by vineyard producers through the growing season, as the total proportion of the infections of over-wintered ascospore is a critical factor in determining the outbreak of conidia over an entire season. Nonetheless, skillful protection of grapevines by contact, translaminar, or systemic fungicides also helps to address unexplained uncertainty and current shortcomings of the model-based forecasts.

Author Contributions: N.K.N. co-supervised the lead author/PhD student (W.L.), primarily funded the research, co-designed and co-developed the model, and contributed to preparation/editing of the manuscript. W.L. co-designed and co-developed the model, implementing it using the R Statistical Language, synthesized model results, and contributed to preparation and editing of the manuscript. W.L. is a PhD/Doctoral Candidate with the University of Victoria and also a Research Affiliate with the Government of Canada/AAFC working from the Summerland Research and Development Centre. D.E.A. was the university co-supervisor of W.L. and contributed to the design and development of the model and preparation and editing of the manuscript. O.C. advised on

the model design, provided vineyard data for training and validating the model and contributed to preparation and editing of the manuscript. A.J.C. advised on use of climate and weather forecast data and model sensitivity and validation, and edited a manuscript draft. All authors have read and agreed to the published version of the manuscript.

Funding: This research was supported by funding awarded to OC and NKN under the Canadian Agricultural Partnerships (CAP) program (AAFC), Project #2336 (J0001792.001.08); Influence of cultural practices and climate change on sustainability of grape production under northern conditions. W.L. was an AAFC Research Affiliate (RAP) funded through this research grant. DEA was supported by NSERC discovery grant funding and AC by Environment and Climate Change Canada (ECCC) research funding.

Conflicts of Interest: The authors declare no conflict of interest.

References

1. Rimerman, F. *The Economic Impact of the Wine and Grape Industry in Canada 2015*; Frank Rimerman + Co. LPP., The Wine Business Center: St. Helena, CA, USA, 2015. Available online: http://www.canadianvintners.com/wp-content/uploads/2017/06/Canada-Economic-Impact-Report-2015.pdf (accessed on 24 April 2020).
2. Carisse, O. Development of grape downy mildew (*Plasmopara viticola*) under northern viticulture conditions: influence of fall disease incidence. *Eur. J. Plant Pathol.* **2016**, *144*, 773–783. [CrossRef]
3. Dereudre, J.; Audran, J.; Leddet, C.; Ait Barka, E.; Brun, O. Réponse de la vigne (*Vitis vinifera* L.) Aux Températures Inférieures à 0 °C; III: Eff. D'un Refroidissement Contrôlé Sur Des Bourgeons En Cours De Débourrement. *Agronomy* **1993**, *13*, 509–514. [CrossRef]
4. Pirrello, C.; Mizzotti, C.; Tomazetti, T.C.; Colombo, M.; Bettinelli, P.; Prodorutti, D.; Peressotti, E.; Zulini, L.; Angeli, G.; Stefanini, M.; et al. Emergent Ascomycetes in viticulture: An interdisciplinary overview. *Front. Plant Sci.* **2019**, *10*, 1394. [CrossRef] [PubMed]
5. Calonnec, A.; Cartolaro, P.; Poupot, C.; Dubourdieu, D.; Darriet, P. Effects of *Uncinula necator* Yield Qual. Grapes (*Vitis vinifera*) Wine. *Plant Pathol.* **2004**, *53*, 434–445. [CrossRef]
6. Gadoury, D.M.; Seem, R.C.; Pearson, R.C.; Wilcox, W.F.; Dunst, R.M. Effects of powdery mildew on vine growth, yield, and quality of concord grapes. *Plant Dis.* **2001**, *85*, 137–140. [CrossRef]
7. Pool, W. Moves towards a Common Market in insurance. *Common Mark. Law Rev.* **1984**, *21*, 123–147.
8. Ficke, A.; Gadoury, D.M.; Seem, R.C. Ontogenic resistance and plant disease management: A case study of grape powdery mildew. *Phytopathology* **2002**, *92*, 671–675. [CrossRef]
9. Gadoury, D.M.; Seem, R.C.; Ficke, A.; Wilcox, W.F. Ontogenic resistance to powdery mildew in grape berries. *Phytopathology* **2003**, *93*, 547–555. [CrossRef]
10. Valdés-Gómez, H.; Gary, C.; Cartolaro, P.; Lolas-Caneo, M.; Calonnec, A. Powdery mildew development is positively influenced by grapevine vegetative growth induced by different soil management strategies. *Crop Prot.* **2011**, *30*, 1168–1177. [CrossRef]
11. Gadoury, D.M.; Seem, R.C.; Ficke, A.; Wilcox, W.F. The epidemiology of powdery mildew on Concord grapes. *Phytopathology* **2001**, *91*, 948–955. [CrossRef]
12. Gadoury, D.M.; Cadle-Davidson, L.; Wilcox, W.F.; Dry, I.B.; Seem, R.C.; Milgroom, M.G. Grapevine powdery mildew (*Erysiphe necator*): A fascinating system for the study of the biology, ecology, and epidemiology of an obligate biotroph. *Mol. Plant Pathol.* **2012**, *13*, 1–16. [CrossRef] [PubMed]
13. Gadoury, D.M.; Pearson, R.C. Initiation, development, dispersal and survival of cleistothecia of *Uncinula necator* New York Vineyards. *Phytopathology* **1988**, *78*, 1413–1421. [CrossRef]
14. Gadoury, D.M.; Pearson, R.C. Ascocarp dehiscence and ascospore discharge in *Uncinula necator*. *Phytopathology* **1990**, *80*, 393–401. [CrossRef]
15. Gadoury, D.M.; Pearson, R.C. Germination of ascospores and infection of Vitis by *Uncinula necator*. *Phytopathology* **1990**, *80*, 1198–1203. [CrossRef]
16. Cortesi, P.; Bisiach, M.; Ricciolini, M.; Gadoury, D.M. Cleistothecia of Uncinula necator—An additional source of inoculum in Italian vineyards. *Plant Dis.* **1997**, *81*, 922–926. [CrossRef] [PubMed]
17. Jailloux, F.; Willocquet, L.; Chapuis, L.; Froidefond, G. Effect of weather factors on the release of ascospores of *Uncinula necator*, Cause Grape Powdery Mildew, Bordx. *Reg. Can. J. Bot.* **1999**, *77*, 1044–1051.
18. Willocquet, L.; Clerjeau, M. An analysis of the effects of environmental factors on conidial dispersal of *Uncinula necator* (grape Powdery Mildew) Vineyards. *Plant Pathol.* **1998**, *47*, 227–233. [CrossRef]

19. Willocquet, L.; Berud, F.; Raoux, L.; Clerjeau, M. Effects of wind, relative humidity, leaf movement and colony age on dispersal of conidia of *Uncinula necator*, Causal Agent Grape Powdery Mildew. *Plant Pathol.* **1998**, 47, 234–242. [CrossRef]
20. Willocquet, L.; Colombet, D.; Rougier, M.; Fargues, J.; Clerjeau, M. Effects of Radiation, Especially Ultraviolet B, on Conidial Germination and Mycelial Growth of Grape Powdery Mildew. *Eur. J. Plant Pathol.* **1996**, *102*, 441–449. [CrossRef]
21. Carisse, O.; Bacon, R.; Lefebvre, A.; Lessard, K. A degree-day model to initiate fungicide spray programs for management of grape powdery mildew (*Erysiphe necator*). *Can. J. Plant Pathol.* **2009**, *31*, 186–194. [CrossRef]
22. Carisse, O.; Bacon, R.; Lefebvre, A. Grape powdery mildew (*Erysiphe necator*) Risk Assess. Based Airborne Conidium Conc. *Crop Prot.* **2009**, *28*, 1036–1044. [CrossRef]
23. Delp, C.J. Effect of temperature and humidity on the grape powdery mildew fungus. *Phytopathology* **1954**, *44*, 615–626.
24. Carroll, J.; Wilcox, W. Effects of humidity on the development of grapevine powdery mildew. *Phytopathology* **2003**, *93*, 1137–1144. [CrossRef] [PubMed]
25. Chellemi, D.O.; Marois, J.J. Development of a demographic growth model for *Uncinula necator* Using A Microcomput. Spreadsheet Program. *Phytopathology* **1991**, *81*, 250–254. [CrossRef]
26. Caffi, T.; Rossi, V.; Legler, S.E.; Bugiani, R. A mechanistic model simulating ascosporic infections by *Erysiphe necator*, Powdery Mildew Fungus Grapevine. *Plant Pathol.* **2011**, *60*, 522–531. [CrossRef]
27. Calonnec, A.; Cartolaro, P.; Naulin, J.M.; Bailey, D.; Langlais, M. A host-pathogen simulation model: Powdery mildew of grapevine. *Plant Pathol.* **2008**, *57*, 493–508. [CrossRef]
28. Hamill, T.M.; Bates, G.T.; Whitaker, J.S.; Murray, D.R.; Fiorino, M.; Galarneau, T.J., Jr.; Zhu, Y.; Lapenta, W. NOAA's second-generation global medium-range ensemble reforecast dataset. *Bull. Am. Meteorol. Soc.* **2013**, *94*, 1553–1565. [CrossRef]
29. Miller, P.; Lanier, W.; Brandt, S. *Using Growing Degree Days to Predict Plant Stages*; Ag/Extension Communications Coordinator, Communications Services, Montana State University-Bozeman: Bozeman, MO, USA, 2001; pp. 1–2.
30. Yang, S.; Logan, J.; Coffey, D.L. Mathematical formulae for calculating the base temperature for growing degree days. *Agric. For. Meteorol.* **1995**, *74*, 61–74. [CrossRef]
31. McMaster, G.S.; Wilhelm, W. Growing degree-days: One equation, two interpretations. *Agric. For. Meteorol.* **1997**, *87*, 291–300. [CrossRef]
32. Jones, G.V.; Davis, R.E. Climate influences on grapevine phenology, grape composition, and wine production and quality for Bordeaux, France. *Am. J. Enol. Vitic.* **2000**, *51*, 249–261.
33. Reid, K.E.; Olsson, N.; Schlosser, J.; Peng, F.; Lund, S.T. An optimized grapevine RNA isolation procedure and statistical determination of reference genes for real-time RT-PCR during berry development. *BMC Plant Biol.* **2006**, *6*, 27. [CrossRef] [PubMed]
34. Analytis, S. Über die Relation zwischen biologischer Entwicklung und Temperatur bei phytopathogenen Pilzen. *J. Phytopathol.* **1977**, *90*, 64–76. [CrossRef]
35. Analytis, S. Obtaining of sub-models for modeling the entire life cycle of a pathogen/Über die Erlangung von Sub-Modellen, die zur Beschreibung eines gesamten Lebenszyklus eines Krankheitserregers dienen. *J. Plant Dis. Prot.* **1980**, 371–382.
36. Rossi, V.; Caffi, T.; Legler, S.E. Dynamics of ascospore maturation and discharge in *Erysiphe necator*, Causal Agent Grape Powdery Mildew. *Phytopathology* **2010**, *100*, 1321–1329. [CrossRef]
37. Gessler, C.; Blaise, P. An extended progeny/parent ratio model II. Application to experimental data. *J. Phytopathol.* **1992**, *134*, 53–62. [CrossRef]
38. Sall, M.A. Epidemiology of grape powdery mildew: A model. *Phytopathology* **1980**, *70*, 338–342. [CrossRef]
39. Verma, T.; Pearl, J. *Equivalence and Synthesis of Causal Models*; UCLA, Computer Science Department: Los Angeles, CA, USA, 1991.
40. Margaritis, D. *Learning Bayesian Network Model Structure from Data*; Technical Report; Carnegie-Mellon Univ Pittsburgh Pa School of Computer Science: Pittsburgh, PA, USA, 2003.
41. Tsamardinos, I.; Aliferis, C.F.; Statnikov, A.R.; Statnikov, E. Algorithms for Large Scale Markov Blanket Discovery. In Proceedings of the FLAIRS Conference, St. Augustine, FL, USA, 12–14 May 2003; Volume 2, pp. 376–380.

42. Yaramakala, S.; Margaritis, D. Speculative Markov blanket discovery for optimal feature selection. In Proceedings of the Fifth IEEE International Conference on Data Mining (ICDM'05), Houston, TX, USA, 27–30 November 2005; p. 4.
43. Mammeri, Y.; Burie, J.B.; Langlais, M.; Calonnec, A. How changes in the dynamic of crop susceptibility and cultural practices can be used to better control the spread of a fungal pathogen at the plot scale? *Ecol. Model.* **2014**, *29*, 178–191. [CrossRef]
44. Burie, J.B.; Langlais, M.; Calonnec, A. Switching from a mechanistic model to a continuous model to study at different scales the effect of vine growth on the dynamic of a powdery mildew epidemic. *Ann. Bot.* **2011**, *107*, 885–895. [CrossRef]